

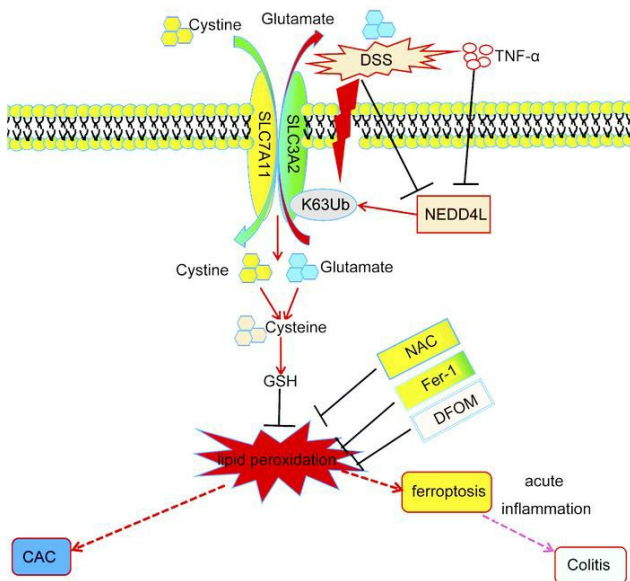
NEDD4L mediates intestinal epithelial cell ferroptosis to restrict inflammatory bowel diseases and colorectal tumorigenesis

Jingjing Liang, ... , Xiaojian Wang, Wenlong Lin

J Clin Invest. 2024. <https://doi.org/10.1172/JCI173994>.

Research In-Press Preview Cell biology Inflammation

Graphical abstract



Find the latest version:

<https://jci.me/173994/pdf>



1 **NEDD4L mediates intestinal epithelial cell ferroptosis to**
2 **restrict inflammatory bowel diseases and colorectal**
3 **tumorigenesis**

4 Jingjing Liang^{1#}, Ning Wang^{1#}, Yihan Yao^{1#}, Yingmei Wang², Xiang An¹, Haofei Wang¹,
5 Huan Liu³, Yu Jiang⁴, Hui Li⁵, Xiaoqing Cheng⁶, Jiaqi Xu⁶, Xiaojing Liang⁷, Jun Lou⁷,
6 Zengfeng Xin¹, Ting Zhang^{8*}, Xiaojian Wang^{1*}, Wenlong Lin^{1*}

7
8 ¹The Second Affiliated Hospital, Zhejiang University School of Medicine, Hangzhou, China;
9 School of Medicine, Hangzhou City University, Hangzhou, China

10 ²State Key Laboratory of Cancer Biology, Department of Pathology, Xijing Hospital and
11 School of Basic Medicine, the Fourth Military Medical University, Xi'an, China

12 ³Institute of Basic and Translational Medicine, Xi'an Medical University, Xi'an, China,

13 ⁴Department of Clinical Laboratory Medicine, Second Affiliated Hospital, School of
14 Medicine, Zhejiang University, Hangzhou, China.

15 ⁵Department of Medical Oncology, the Cancer Hospital of the University of Chinese
16 Academy of Sciences (Zhejiang Cancer Hospital);

17 ⁶Department of Pathology, Sir Run Run Shaw Hospital, Zhejiang University School of
18 Medicine, Hangzhou, China.

19 ⁷Department of Respiratory and Critical Medicine, Sir Run Run Shaw Hospital, Zhejiang
20 University, School of Medicine, Hangzhou, China

21 ⁸Department of Radiation Oncology, The Second Affiliated Hospital, Zhejiang University
22 School of Medicine, Hangzhou, China

23 #These authors contributed equally.

24 *Address correspondence to: Wenlong Lin, Zhejiang University, 866 Yuhang Tang Road,
25 Hangzhou, Zhejiang, P. R. China. Phone: 86.0571.88981662; Email: lwl210@foxmail.com.

26 Or to: Xiaojian Wang, Zhejiang University, 866 Yuhang Tang Road, Hangzhou, Zhejiang, P.
27 R. China; Phone: 86.0571.88201220; Email: wangxiaojian@cad.zju.edu.cn. Or to: Ting
28 Zhang, The Second Affiliated Hospital, Zhejiang University School of Medicine, Zhejiang,
29 P. R. China; Phone: 86.0571. 87783521; Email: zezht@zju.edu.cn.

30

31

32

33

34

35

36

37

38

39

40

41

42

43

44

45 **Abstract**

46 Various factors play key roles in maintaining intestine homeostasis. Disruption of the
47 balance may lead to intestinal inflammatory diseases (IBDs) and even colorectal cancer
48 (CRC). Loss or gain of function of many key proteins can result in dysregulated intestinal
49 homeostasis. Our research demonstrated that neural precursor cells expressed
50 developmentally down-regulated 4-like protein (NEDD4L or NEDD4-2), a type of HECT
51 family E3 ubiquitin ligase, played an important role in maintaining intestinal homeostasis.
52 NEDD4L expression was significantly inhibited in intestinal epithelial cells (IECs) of patients
53 with Crohn's disease (CD), ulcerative colitis (UC), and CRC. Global knockout of NEDD4L
54 or its deficiency in IECs exacerbated dextran sulfate sodium (DSS)-/2,4,6-trinitrobenzene
55 sulfonic acid (TNBS)-induced colitis and azoxymethane (AOM)/DSS-induced colorectal
56 cancer. Mechanistically, NEDD4L deficiency in IECs inhibited the key ferroptosis regulator
57 glutathione peroxidase 4 (GPX4) expression by reducing the protein expression of solute
58 carrier family 3 member 2 (SLC3A2) without affecting its gene expression, ultimately
59 promoting DSS-induced IEC ferroptosis. Importantly, ferroptosis inhibitors reduced the
60 susceptibility of NEDD4L-deficient mice to colitis and colitis-associated colorectal cancer
61 (CAC). Thus, NEDD4L is an important regulator in IEC ferroptosis, maintaining intestinal
62 homeostasis, making it a potential clinical target for diagnosing and treating IBDs.

63

64

65

66

67 **Introduction**

68 The intestinal mucosa is the largest mucosal surface that communicates with the
69 environment, dietary antigens, and various microorganisms, serving as a critical
70 component of immune regulation(1, 2). The intestinal mucosal barrier, composed of the
71 intestinal epithelial cells (IECs), the immune barrier, and the intestinal flora barrier (3),
72 jointly maintains intestinal homeostasis. Intestinal disorders caused by various factors such
73 as diet, genetic susceptibility, environmental factors, and mucosal immune disorders
74 contribute to the development of intestinal diseases, including colitis and colorectal cancer
75 (CRC)(4). Therefore, maintaining intestinal mucosa homeostasis is crucial for controlling
76 inflammation and preventing excessive immunopathology following inflammation.

77 Inflammatory bowel diseases (IBDs), including Crohn's disease (CD) and ulcerative
78 colitis (UC), are complicated diseases characterized by abnormal mucosal immune
79 responses triggered by microorganisms, cytokines, and damaged epithelial cells, which
80 can exacerbate the inflammation during the pathogenesis of colitis(4). Ferroptosis, a kind
81 of cell death induced by excessive ferric ion levels and lipid peroxidation, exhibits a distinct
82 morphology from other forms of cell death, such as apoptosis, necroptosis, and pyroptosis.
83 Playing a crucial role in a variety of tissues and cell types, including neuron cells, renal
84 tubular epithelial cells, endothelial cells, and T cells (5, 6), ferroptosis regulates diseases
85 associated with cell death. Proteins like glutathione peroxidase 4 (GPX4), solute carrier
86 family 7 member 3 (SLC7A11), solute carrier family 3 member 2 (SLC3A2), and others
87 directly or indirectly participate in the regulation of ferroptosis (5, 7). The ferroptosis of
88 many tumor cells can be modulated by adjusting the expression levels of GPX4, SLC7A11,

89 and intracellular lipid peroxidation (8). However, only a few studies have reported on
90 ferroptosis in intestine homeostasis (9, 10), and the regulatory function of SLC3A2 in
91 ferroptosis remains largely unclear (11).

92 Numerous key proteins play important roles in maintaining the homeostasis of IECs
93 (12, 13). E3 ubiquitin ligases, such as TNF alpha induced protein 3 (TNFAIP3, A20),
94 baculoviral IAP repeat containing 2 (BIRC2, cIAP1), baculoviral IAP repeat containing 3
95 (BIRC3, cIAP2), tripartite motif containing 31 (TRIM31), ring finger protein 186 (RNF186),
96 and membrane associated ring-CH-type finger 3 (MARCH3), serve as key negative
97 regulators in multiple signal pathways, participating in intestinal homeostasis by regulating
98 immune response, intestinal epithelial cell proliferation, apoptosis, or necroptosis(14-20).
99 Neural precursor cells expressed developmentally down-regulated 4-like protein
100 (NEDD4L), a member of the E3 ubiquitin ligase HECT family, is essential for maintaining
101 cell homeostasis as it can bind and regulate a variety of membrane proteins (21). NEDD4L
102 has an amino-terminal Ca^{2+} phospholipid binding (C2) domain, a protein-protein interaction
103 (WW) domain, and a HECT domain located at the carboxyl-terminal (22). The most clearly
104 studied target of NEDD4L is the epithelial sodium channel (ENaC), which is usually
105 expressed in lung and kidney epithelial cells, participating in related diseases (23-25). It
106 also mediates the polyubiquitination and degradation of Smad2/3, thereby limiting the TGF-
107 β signaling pathway (26). However, the regulatory role of NEDD4L in IBDs and colitis-
108 associated colorectal cancer (CAC) remains unclear (27).

109 Here, we identified that both the gene and protein expression of NEDD4L were
110 significantly inhibited in the IECs of patients with colitis and CRC, and negatively correlated

111 with the disease status of colitis. NEDD4L deficiency in mice promoted dextran sulfate
112 sodium (DSS)-/2,4,6-trinitrobenzene sulfonic acid (TNBS)-induced colitis and
113 azoxymethane (AOM)/DSS-induced colorectal cancer. Mechanistically, NEDD4L
114 deficiency in IECs reduced the protein expression of the soluble amino acid transport
115 protein SLC3A2 without affecting its gene expression. This led to the inhibition of the key
116 ferroptosis regulator GPX4 expression, ultimately promoting DSS-induced IEC ferroptosis.
117 Importantly, ferroptosis inhibitors, such as ferrostatin-1 (Fer-1) and deferoxamine mesylate
118 (DFOM), reversed the colitis and CAC phenotype difference between wild-type (WT) and
119 NEDD4L IEC-deficient (*Nedd4l^{fl/fl} Villin^{Cre}*) mice. Collectively, our data demonstrated that
120 NEDD4L acted as an important regulator in IEC ferroptosis, thus maintaining intestinal
121 homeostasis and controlling the development of colitis and CAC, suggesting that NEDD4L
122 might be a potential target for the diagnosis and treatment of these diseases.

123

124

125

126

127

128

129

130

131

132

133 **Results**

134 **NEDD4L expression is inhibited in IBDs**

135 Our previous data have demonstrated that NEDD4L plays a crucial role in IL-17-, IL-6-, and
136 viruses-mediated innate immune responses (28-30). However, its role in intestinal
137 homeostasis remains unclear. To explore the potential function of NEDD4L in intestinal
138 homeostasis, we first analyzed the *NEDD4L* gene expression in the public database. As
139 shown in Supplementary Figure 1, A and B, the *NEDD4L* gene was highly expressed in
140 human neuron, lung, and intestinal systems, particularly highest in goblet cells, but was
141 lowly expressed in the human immune system, indicating that highly expressed *NEDD4L*
142 in intestinal epithelium might be involved in maintaining intestinal homeostasis. We
143 analyzed the gene expression of *NEDD4L* in patients with IBDs from GEO datasets. As
144 shown in Supplementary Figure 1, C-E, compared to the healthy control (HC), *NEDD4L*
145 gene expression in colonic mucosa was restricted in patients with CD and UC.
146 Nevertheless, *NEDD4L* gene expression was significantly increased in PBMCs from
147 patients with CD and UC compared with HC (Supplementary Figure 1F). Two cohorts of
148 study subjects from the Xijing Hospital (cohort1) and First Affiliated Hospital of Zhejiang
149 University, School of Medicine (FAHZU, cohort2) were recruited to trace the NEDD4L
150 protein expression in the colonic biopsies. As shown in Figure 1, A-D, the NEDD4L protein
151 level in IECs was significantly reduced in patients with UC and CD compared to the normal
152 control subjects (HC). In the samples from cohort1, only 4.8% of the biopsies from patients
153 with UC (4/83) exhibited strong NEDD4L immunohistochemistry (IHC) staining, whereas
154 20% of the healthy control subjects (8/40) showed strong NEDD4L IHC staining ($p < 0.001$;

155 table 1). Similar results were observed in cohort2, only 38.8% of the UC patient biopsies
156 (14/36) and 39.0% of the CD patient biopsies (16/41) exhibited strong NEDD4L IHC
157 staining, whereas 96.8% of the healthy control subjects (30/31) showed strong NEDD4L
158 IHC staining ($p < 0.001$; table 2). Importantly, NEDD4L protein expression was lower in
159 patients with moderate or severe colitis than in those with mild colitis from cohort2 (Figure
160 1, E and F), consistent with the GEO data (Supplementary Figure 1G), indicating that
161 NEDD4L expression was negatively correlated with the severity of colitis. Similarly,
162 *NEDD4L* gene expression in colonic mucosa was significantly inhibited in the diseased
163 individual from monozygotic twin pairs discordant for ulcerative colitis compared to the
164 healthy individual (Supplementary Figure 1H), suggesting that the reduced expression of
165 *NEDD4L* was likely to be a consequence of IEC damage or inflammation. To further explore
166 the specific expression profile of *NEDD4L* in IECs, a single-cell RNA analysis was
167 performed. Compared to the healthy tissue, the gene expression of *NEDD4L* in inflamed
168 colon tissues from patients with UC was significantly inhibited in enterocytes (including
169 bestrophin 4 (Best4)⁺ enterocytes, immature enterocytes2), goblet, transit-amplifying cell
170 (TA, including TA1, TA2, cycling TA, and secretory TA), stem cells, but not significantly
171 changed in enterocytes progenitors, enteroendocrine, immature enterocytes1, M cells, and
172 tuft cells (Supplementary Figure 1I). Furthermore, both the gene and protein expression of
173 NEDD4L in patients with IBDs were significantly inhibited compared to the normal colon
174 mucosa (Figure 1, G and H). Additionally, upon DSS treatment in mice, both the gene and
175 protein expression of NEDD4L in IECs were significantly inhibited (Figure 1, I and J and
176 Supplementary Figure 1, J and K). Collectively, these results suggest that the NEDD4L

177 gene and protein were significantly inhibited in humans and mice with colitis, and NEDD4L
178 expression was correlated with the severity of patients with IBDs.

179 ***Nedd4l* deficiency in mice enhances sensitivity to experimental colitis**

180 To investigate the role of NEDD4L in colitis, *Nedd4l* heterozygous knockout mice
181 (*Nedd4l*^{+/-}) and control wild-type littermates (*Nedd4l*^{+/+}) were initially challenged with 4%
182 DSS to induce an acute experimental colitis model. The mortality rate was significantly
183 higher in *Nedd4l*^{+/-} mice compared to *Nedd4l*^{+/+} mice (Figure 2A). Remarkably, we
184 observed more severe colitis after 3% DSS treatment in *Nedd4l*^{+/-} mice compared to
185 *Nedd4l*^{+/+} mice, as evidenced by significantly greater body weight loss, higher rectal
186 bleeding score, and shorter colons in DSS-treated *Nedd4l*^{+/-} mice (Figure 2, B-F).
187 Furthermore, *Nedd4l* global deficient mice (*Nedd4l*^{-/-}, KO) exhibited a more severe colitis
188 phenotype when treated with a very low dosage of DSS (1%), which was hard to induce
189 obvious colitis phenotype in *Nedd4l*^{+/-} and *Nedd4l*^{+/+} mice, suggesting that *Nedd4l* knockout
190 increased the susceptibility of mice to low-dose DSS exposure (Supplementary Figure 2,
191 A-E).

192 To determine whether *Nedd4l* deficiency in IECs or hematopoietic cells contributes to
193 the more severe colitis phenotype, bone marrow chimera experiments were conducted.
194 Lethally irradiated *Nedd4l*^{+/+}(WT) and *Nedd4l*^{-/-}(KO) mice were reconstituted with bone
195 marrow cells from WT mice. Mice reconstituted with *Nedd4l* deficiency in non-
196 hematopoietic cells (WT→KO) exhibited a more severe colitis phenotype compared to the
197 *Nedd4l*^{+/+} chimeras (WT→WT) following DSS treatment (Figure 2, G-J). Collectively, these
198 data implicate that NEDD4L in non-hematopoietic cells promoted the pathogenesis of DSS-

199 induced colitis.

200 ***Nedd4l* deficiency in IECs exacerbates DSS-induced and TNBS-induced**
201 **experimental colitis**

202 To further explore whether the protective role of NEDD4L in colitis was intrinsic to IECs, we
203 generated IEC-specific *Nedd4l* knockout mice (*Nedd4l^{fl/fl} Villin^{Cre}*) by crossing *Nedd4l* floxed
204 mice (*Nedd4l^{fl/fl}*) with *Villin^{Cre}* mice, resulting in constitutive deletion of *Nedd4l* in the IECs.

205 Consistent with previous reports (31), *Nedd4l^{fl/fl} Villin^{Cre}* mice displayed normal intestinal
206 histology. The terminally differentiated cells were indistinguishable between wild-type and
207 *Nedd4l^{fl/fl} Villin^{Cre}* mice under steady-state conditions (Supplementary Figure 2, F and G).

208 In addition, assessment of the numbers of goblet cells, Paneth cells, enteroendocrine, and
209 enterocytes (identified by periodic acid–Schiff (PAS), lysozyme (Lyz), chromogranin A
210 (ChgA), and alkaline phosphatase (ALP) staining, respectively) revealed no obvious
211 difference in terms of cell lineage commitment (Supplementary Figure 2, F-I). This

212 observation was further confirmed by qPCR analysis, which showed no significant
213 alterations in the expression of marker genes for the different cell lineages and stem cell
214 populations in intestinal tissue from *Nedd4l^{fl/fl} Villin^{Cre}* mice compared with control *Nedd4l^{fl/fl}*

215 mice (Supplementary Figure 2, J and K). However, *Nedd4l^{fl/fl} Villin^{Cre}* mice showed a
216 significantly higher death rate than control littermates upon 2.5% DSS treatment (Figure
217 3A). *Nedd4l^{fl/fl} Villin^{Cre}* mice exhibited more severe weight loss, rectal bleeding, colon

218 shortening, epithelial damage, and crypt architecture disruption than *Nedd4l^{fl/fl}* mice when
219 challenged with 2% DSS (Figure 3, B-F). Additionally, a 5-day DSS treatment induced

220 comparable degrees and absolute cell numbers of mucous-infiltrated monocytes,

221 macrophages, and neutrophils, but increased absolute cell numbers of mucous-infiltrated
222 T cells and B cells in *Nedd4^{fl/fl} Villin^{Cre}* mice compared with the control littermates (Figure
223 3G). Moreover, following the development of colitis, particularly on day 9, much more
224 inflammatory immune cell infiltration in mucous was observed in *Nedd4^{fl/fl} Villin^{Cre}* mice
225 compared to *Nedd4^{fl/fl}* mice, including monocytes, macrophages, T cells, and B cells
226 (Figure 3H).

227 We then investigated whether *Nedd4l* deficiency might exacerbate colitis in an
228 alternative model induced by TNBS. As expected, compared with the control group, TNBS-
229 treated *Nedd4^{fl/fl} Villin^{Cre}* mice phenocopied the aggravated symptoms of colitis as in DSS-
230 treated *Nedd4^{fl/fl} Villin^{Cre}* mice (Supplemental Figure 3, A-F). Collectively, these data
231 support the notion that *Nedd4l* deficiency in IECs contributed both to DSS-induced and
232 TNBS-induced colonic damage and colitis.

233 ***Nedd4l* deficiency in IECs promotes IEC ferroptosis and subsequent intestinal** 234 **barrier integrity damage**

235 To explore the underlying mechanisms of NEDD4L in regulating colitis, colonic tissues from
236 DSS-treated *Nedd4^{fl/fl} Villin^{Cre}* mice and *Nedd4^{fl/fl}* littermates were subjected to RNA-
237 sequencing analysis. As shown in Figure 4A, the tight junction signaling was significantly
238 downregulated in *Nedd4^{fl/fl} Villin^{Cre}* mice compared to *Nedd4^{fl/fl}* littermates. Furthermore,
239 the *Nedd4^{fl/fl} Villin^{Cre}* mice displayed higher serum FITC-dextran concentrations after DSS
240 treatment than *Nedd4^{fl/fl}* mice, while displaying similar epithelial permeability to *Nedd4^{fl/fl}*
241 mice in the absence of DSS treatment (Figure 4B). Additionally, histopathological analysis,
242 tight junction protein 1 (ZO-1) immunofluorescence (IF) staining showed that *Nedd4l*

243 deficiency led to a more severe diminished expression of ZO-1 in the mucosal epithelium
244 in response to DSS treatment (Figure 4C).

245 To further explore the regulation of barrier integrity during the induction of colitis by
246 IEC-derived *Nedd4l*, the IECs from *Nedd4l^{ff/ff} Villin^{Cre}* mice and *Nedd4l^{ff/ff}* littermates with or
247 without DSS treatment were subjected to quantitative ubiquitination mass spectrometry
248 (MS) analysis. As shown in Supplemental Figure 4A, the Gene Ontology (GO) analysis
249 showed that the marked changed potential substrates mainly regulated protein localization,
250 transport, and transport activity. The Kyoto Encyclopedia of Genes and Genomes (KEGG)
251 analysis showed that protein digestion and absorption, mineral absorption, and ferroptosis
252 signaling pathways were markedly enriched in IECs from *Nedd4l^{ff/ff} Villin^{Cre}* mice compared
253 to *Nedd4l^{ff/ff}* mice (Figure 4D and Supplemental Figure 4B). In comparison with WT
254 littermates, the levels of TUNEL-positive epithelial cells, as well as the lipid peroxidation
255 measured by 4 hydroxynonenal (4-HNE)-positive staining cells, and malondialdehyde
256 (MDA) contents, were remarkably enhanced in DSS-treated *Nedd4l^{ff/ff} Villin^{Cre}* mice,
257 suggesting that *Nedd4l* deficiency in IECs promoted the lipid peroxidation-mediated IEC
258 death after DSS treatment (Figure 4, E-I). IECs from *Nedd4l^{ff/ff} Villin^{Cre}* mice exhibited much
259 more severe ferroptosis morphology, characterized by mitochondrial fragmentation, the
260 disappearance of internal cristae and collapse, compared with *Nedd4l^{ff/ff}* mice (Figure 4J).
261 Consistently, the expression levels of ferroptosis and pro-inflammatory-related genes, such
262 as *Gpx4*, were significantly restricted in *Nedd4l^{ff/ff} Villin^{Cre}* mice relative to *Nedd4l^{ff/ff}* mice,
263 while the gene expression levels of transferrin receptor protein 1 (*TfR1*, also known as
264 *Tfrc*), prostaglandin-endoperoxide synthase 2 (*Ptgs2*), and lipocalin 2 (*Lcn2*) were

265 significantly increased in *Nedd4^{fl/fl} Villin^{Cre}* mice (Supplemental Figure 4, C and D).
266 Furthermore, we stimulated the intestine organoids derived from *Nedd4^{fl/fl} Villin^{Cre}* mice and
267 *Nedd4^{fl/fl}* mice with DSS and ferroptosis inducers in vitro, including Erastin, Erastin2 (a
268 specific glutamine/cystine transporter inhibitor), and RSL3, to check if NEDD4L could
269 mediate IEC ferroptosis. As shown in Figure 4, K and L, *Nedd4l* deficiency in IECs
270 promoted lipid peroxidation-mediated IEC death, which was assessed by 4',6-diamidino-
271 2-phenylindole (DAPI, indicating the dead cell) and fluorescein isothiocyanate (FITC)-
272 BODIPY C11 staining (indicating intercellular lipid peroxidation production). Our data
273 suggest that NEDD4L maintained intestinal barrier integrity by inhibiting IEC ferroptosis.

274 We have noticed that the expression of both the NEDD4L gene and protein were
275 inhibited during the induction of colitis by DSS treatment in mice, indicating that DSS-
276 induced IEC ferroptosis may be a potential inducer of the inhibition of NEDD4L expression
277 during the colitis. Thus, ferroptosis inducers, including Erastin and RSL3, were employed
278 to clarify the role of ferroptosis in NEDD4L expression. As shown in Supplemental Figure
279 4, E and F, Erastin and RSL3 significantly inhibited the NEDD4L protein expression,
280 suggesting that cell ferroptosis may regulate NEDD4L expression. What's more, other
281 classical cell death, TNF- α plus CHX-induced epithelial cell pyroptosis, and staurosporine-
282 induced cell apoptosis inhibited the NEDD4L expression, except for insensitive necroptosis
283 in HCT116 cells induced by T/S/Z (32-35) (Supplemental Figure 4, G and H). The key
284 cytokines involved in colitis, such as TNF- α , IL-17A, and IL-1 α , were employed to test if
285 DSS-induced downstream cytokines restricted the NEDD4L expression. As shown in
286 Supplemental Figure 4, I and J, TNF- α , but not IL-17A or IL-1 α , restricted NEDD4L

287 expression in HCT116 cells along with NF- κ B P65 subunit phosphorylation, indicating that
288 TNF- α serves as the key mediator for inhibiting NEDD4L expression in IECs. Collectively,
289 our data demonstrate that IEC death induced by the DSS, Erastin, RSL3, and downstream
290 TNF- α inhibited NEDD4L expression.

291 Since DSS and ferroptosis inducers directly inhibited NEDD4L expression in HCT116
292 cells, we tested whether NEDD4L could regulate cell ferroptosis induced by DSS or
293 ferroptosis inducers in vitro. As shown in Supplemental Figure 5, A-E, NEDD4L negatively
294 regulated DSS-induced cell ferroptosis in HCT116 cells in an E3 ligase activity-dependent
295 manner, as assessed by measurement of cell viability, lipid peroxidation, and MDA content.
296 Similar phenotypes were also detected in other cell lines, including SW480 and RKO cells,
297 using a siRNA silencing system (Supplemental Figure 5, F-K). Furthermore, *NEDD4L*
298 deficiency in HCT116, SW480, and RKO cells significantly promoted Erastin- or RSL3-
299 induced cell ferroptosis and lipid peroxidation production (Supplemental Figure 5, L-S).
300 Collectively, these data further confirm that NEDD4L negatively regulated cell death and
301 lipid peroxidation production mediated by DSS and ferroptosis inducers in multiple cell
302 lines, in a manner dependent on its E3 ligase activity.

303 **SLC3A2 is a potential substrate of NEDD4L in DSS-induced colitis**

304 Based on the quantitative ubiquitylation MS analysis, SLC3A2, a transmembrane protein,
305 which forms the key glutamine/cystine transporter with SLC7A11 and consequently
306 participates in ferroptosis, was identified as one of the most remarkably ubiquitinated
307 substrates and was significantly downregulated in *Nedd4^{fl/fl}Villin^{Cre}* IECs compared to that
308 in *Nedd4^{fl/fl}* IECs after DSS challenge. Nevertheless, the fold change of SLC3A2 analyzed

309 by ubiquitylation MS was inhibited due to the reduced NEDD4L expression upon DSS
310 treatment compared with untreated mice (Figure 5, A and B and Supplemental Figure 6, A
311 and B). The interaction MS analysis in Flag-NEDD4L stably expressed HCT116 cells
312 indicated that NEDD4L interacted with SLC3A2 (Figure 5B and Supplemental Figure 6C).
313 Based on the combined analysis of quantitative ubiquitination MS and interaction MS, we
314 hypothesized that NEDD4L might interact with SLC3A2 and regulate its ubiquitination,
315 triggering IEC ferroptosis and aggravating DSS-induced colitis. Consistently, the protein
316 expression of SLC3A2 was significantly downregulated in IECs of *Nedd4^{fl/fl} Villin^{Cre}* mice
317 compared to that of *Nedd4^{fl/fl}* mice (Supplemental Figure 6D). Whereas, *Nedd4l* deficiency
318 in IECs had no effects on the protein expressions of GP130 and MEKK2, which have been
319 identified to be potential substrates of NEDD4L in other cells (29, 30). Furthermore, upon
320 DSS treatment, the expression of SLC3A2 was also downregulated in IECs of *Nedd4^{fl/fl}*
321 *Villin^{Cre}* mice compared to that of *Nedd4^{fl/fl}* mice (Figure 5C). Based on the ubiquitylation
322 MS analysis, we found that NEDD4L protein abundance was positively correlated with
323 SLC3A2 protein abundance, further indicating the probability of SLC3A2 as the potential
324 substrate of NEDD4L (Supplemental Figure 6E). It has been reported that SLC3A2
325 regulates the expression of CyclinD1 in IECs to participate in mouse colitis(36). However,
326 we did not observe any difference in the gene expressions of *Cyclind1* and *Slc3a2* in
327 *Nedd4^{fl/fl} Villin^{Cre}* and *Nedd4^{fl/fl}* mice (Supplemental Figure 6F). In addition, we revealed that
328 *Nedd4l* deficiency in IECs restricted SLC3A2 and GPX4 protein expression (Figure 5, C-
329 E). DSS treatment significantly inhibited the protein expression levels of GPX4, SLC3A2,
330 and NEDD4L. Furthermore, the protein expression levels of both NEDD4L and GPX4 were

331 positively correlated with SLC3A2 in IECs upon DSS treatment (Supplemental Figure 6,
332 G-I). Importantly, the protein expression level of NEDD4L in patients with IBDs was
333 positively correlated with SLC3A2 (Figure 5, F and G).

334 NEDD4L knockout in intestinal organoids and HCT116 cells impaired DSS-induced
335 SLC3A2 and GPX4 expression but increased the TFRC expression, enhancing cell
336 ferroptosis (Figure 5, H and I). NEDD4L positively regulated SLC3A2 and GPX4 protein
337 expression in HCT116 cells in its E3 ubiquitin ligase activity-dependent manner (Figure 6J).
338 Similar results were observed in a multitype of DSS-, Erastin-, or RSL3-treated intestinal
339 cell lines, such as HCT116, SW480, and RKO cells, using a siRNA silencing system (Figure
340 5, K-M and Supplemental Figure 6, J-M).

341 As a potential substrate of NEDD4L in ferroptosis signaling, SLC3A2 was poorly
342 studied (11). Therefore, we determined whether SLC3A2 could regulate cell ferroptosis and
343 signaling transduction mediated by DSS or ferroptosis inducers. As shown in Figure 6, A-I
344 and Supplemental Figure 7, A-I, silencing of endogenous *SLC3A2* significantly promoted
345 cell death and lipid peroxidation production induced by DSS and ferroptosis inducers.
346 Additionally, silencing of endogenous *SLC3A2* inhibited GPX4 expression but enhanced
347 TFRC expression after DSS or ferroptosis inducer treatment compared with scramble
348 siRNA (*siNC*)-transfected cells. Overexpression of exogenous *SLC3A2* in HCT116 cells
349 inhibited DSS-induced cell death and production of lipid peroxidation by upregulating the
350 GPX4 expression (Figure 6, J-M), indicating that SLC3A2 negatively regulated cell
351 ferroptosis mediated by DSS and ferroptosis inducers in vitro. Furthermore,
352 overexpression of the exogenous *SLC3A2* eliminated the difference in DSS-induced cell

353 death, production of lipid peroxidation, and protein expression levels of GPX4 and TFRC
354 between *NEDD4L*-silenced and scramble siRNA (siNC)-transfected HCT116 cells (Figure
355 6, N-P). Collectively, these data suggest that NEDD4L regulated DSS-induced cell
356 ferroptosis through the SLC3A2-GPX4 axis.

357 **NEDD4L mediates SLC3A2 ubiquitination**

358 To determine the mechanism through which NEDD4L orchestrates SLC3A2 protein
359 expression, we investigated the interaction between NEDD4L and SLC3A2 in HCT116 and
360 HEK293T cells. As shown in Figure 7, A and B, NEDD4L interacted dynamically with
361 SLC3A2 upon DSS treatment, peaking at 12 hours. The E3 ligase activity mutant of
362 NEDD4L (NEDD4L-C942A or NEDD4L-CA) abolished this interaction. To map the domains
363 required for NEDD4L to interact with SLC3A2, we constructed a series of plasmids
364 expressing wild-type or mutant NEDD4L, in which C2 (Δ C2), WW (Δ WW), or HECT
365 (Δ HECT) domain was deleted, respectively. As shown in Figure 7C, the deletion of the
366 HECT domain but not the C2 and WW domain disrupted the interaction between NEDD4L
367 and SLC3A2, demonstrating that the HECT domain was necessary for NEDD4L to bind
368 SLC3A2. As an E3 ubiquitin ligase, NEDD4L might regulate the stability of the SLC3A2
369 protein by mediating its ubiquitination. Firstly, we used the ubiquitin (Ub) antibody to
370 immunoprecipitate endogenous Ub to compare the amount of poly-Ub-linked SLC3A2 in
371 WT (sg*NTC*) or NEDD4L knockout (sg*NEDD4L*) HCT116 cells. As shown in Figure 7D,
372 NEDD4L knockout in HCT116 cells impaired the poly-Ub-linked SLC3A2 upon DSS
373 treatment, consistent with the phenotype observed in our ubiquitination MS in IECs. Then,
374 we performed ubiquitination assays in HEK293T cells. As shown in Figure 7E and

375 Supplemental Figure 8A, NEDD4L positively regulated the poly-ubiquitination of SLC3A2.
376 Furthermore, in vitro cell-free ubiquitination assays demonstrated that it was the wild-type
377 NEDD4L protein, but not the NEDD4L-C942A protein, that directly promoted the poly-
378 ubiquitination of SLC3A2 (Figure 7F). Following MG132 treatment, but not bafilomycin A1
379 (Baf A1) treatment, the expression of SLC3A2 in wild-type NEDD4L transfected cells was
380 reduced to the level comparable with that in control or NEDD4L-CA mutant transfected
381 HCT116 cells, suggesting that NEDD4L regulated the stability of SLC3A2 protein by
382 mediating SLC3A2 ubiquitination in a proteasome-dependent manner (Supplemental
383 Figure 8B). Notably, NEDD4L overexpression in HCT116 cells markedly enhanced the
384 protein stability of SLC3A2 compared to that in NEDD4L-C942A or control transfected cells
385 (Supplemental Figure 8C). NEDD4L- Δ HECT completely lost the capability to mediate
386 SLC3A2 ubiquitination (Figure 7G), suggesting that the HECT domain of NEDD4L was
387 critical for its interaction with and ubiquitination of SLC3A2. Furtherly, NEDD4L mainly
388 promoted Lys-63(K63O)-linked poly-ubiquitination of SLC3A2 (Figure 7G), which is
389 consistent with the well-established notion that the C-terminal amino acids determine the
390 ubiquitin chain specificity of the HECT-type E3 ligases and NEDD4 family ligases, including
391 NEDD4L, which exhibit strict specificity towards K63 linkages (37). NEDD4L knockout
392 markedly impaired DSS-induced K63-linked poly-ubiquitination of SLC3A2, but enhanced
393 K48-linked poly-ubiquitination of SLC3A2, resulting in a reduced SLC3A2 protein
394 expression compared to sgNTC HCT116 cells (Figure 7I). Furthermore, NEDD4L promoted
395 K63-linked poly-ubiquitination of SLC3A2 in a dosage-dependent manner and inhibited the
396 K48-linked poly-ubiquitination of SLC3A2 in HEK293T cells (Figure 8J). We also found that

397 SLC3A2 interacted with GPX4. However, NEDD4L neither interacted with nor ubiquitylated
398 GPX4(Supplemental Figure 8, D and E). These data suggest that NEDD4L mediated the
399 K63-linked poly-ubiquitination of SLC3A2, but not of GPX4.

400 ***Nedd4l* deficiency promotes colitis pathogenesis via ferroptosis in mice**

401 To further determine whether NEDD4L regulates colitis through the ferroptosis pathway,
402 colonic tissues from *Nedd4l^{ff/ff}Villin^{Cre}* and *Nedd4l^{ff/ff}* mice treated with DSS were subjected
403 to RNA-sequencing to explore the underlying mechanisms. KEGG analysis revealed that
404 cytokine-cytokine receptor interaction and IL-17 signaling pathway were the top 2
405 pathways up-regulated in colonic tissues from *Nedd4l^{ff/ff}Villin^{Cre}* mice compared to *Nedd4l^{ff/ff}*
406 mice (Supplemental Figure 9A). GO analysis showed that the cellular intrinsic apoptotic
407 signaling and regulation of the hydrogen peroxide metabolic process were significantly
408 upregulated in colonic tissues from *Nedd4l^{ff/ff}Villin^{Cre}* mice compared to *Nedd4l^{ff/ff}* mice
409 (Supplemental Figure 9B), suggesting that cell death and peroxidation may be involved in
410 NEDD4L-mediated colitis. Previous studies have shown that NEDD4L regulated IL-17-
411 induced inflammatory response through MEKK2 (29). Since IL-17R signaling can affect
412 intestinal epithelial cell homeostasis, differentiation, and tumor development(38-40), we
413 tested whether NEDD4L regulates DSS-induced colitis through IL-17R signaling by using
414 an IL-17 neutralizing antibody. As shown in Supplemental Figure 9, C-F, the IL-17
415 neutralizing antibody treatment successfully inhibited DSS-mediated colitis in WT mice but
416 did not eliminate the colitis phenotype difference induced by *Nedd4l* deficiency. Although
417 Syk is known to be a target for NEDD4L in mast cells(41), continual intraperitoneal(*i.p.*)
418 injection of a Syk-specific inhibitor, BAY 61-3606, during colitis induction did not eliminate

419 the colitis phenotype difference between *Nedd4^{ff}Villin^{Cre}* and *Nedd4^{ff}* mice (Supplemental
420 Figure 9, G-J). However, treatment with a lipid peroxidation scavenger, N-acetylcysteine
421 (NAC), significantly attenuated the development of colitis in *Nedd4^{ff} Villin^{Cre}* mice. More
422 importantly, NAC treatment rescued the colitis phenotype in *Nedd4^{ff}Villin^{Cre}* to a
423 comparable level with those in *Nedd4^{ff}* mice (Supplemental Figure 9, K-N).

424 To further explore if NEDD4L regulates colitis via ferroptosis, a ferroptosis-specific
425 inhibitor, ferrostatin-1 (Fer-1), was continual *i.p.* injected during DSS-induced colitis in
426 *Nedd4^{ff}Villin^{Cre}* and *Nedd4^{ff}* mice. As shown in Figure 8, A-J and Supplemental Figure 10,
427 A and B, Fer-1 markedly rescued the colitis phenotype in DSS-induced *Nedd4^{ff}Villin^{Cre}*
428 mice to levels comparable to those in Fer-1-treated *Nedd4^{ff}* mice, as characterized by
429 reduced diarrhea and rectal bleeding, decreased colon shortening, less epithelial damage,
430 and decreased crypt architecture disruption, decreased epithelial cell death, reduced lipid
431 peroxidation production, and decreased inflammatory cytokines, but increased tight
432 junctions. Furthermore, continual *i.p.* injection of Fer-1 during the induction of colitis
433 eliminated the difference in colitis phenotype between *Nedd4^{ff}Villin^{Cre}* and *Nedd4^{ff}* mice.
434 The difference in the expression of ferroptosis-related genes (including *Gpx4*, nuclear
435 receptor coactivator 4 (*Ncoa4*), acyl-CoA synthetase family member 2 (*Acsf2*), and acyl-
436 CoA synthetase long chain family member 4 (*Acs14*)) and proteins (including GPX4,
437 SLC3A2, and TFRC) between *Nedd4^{ff}Villin^{Cre}* and *Nedd4^{ff}* mice were eliminated by the
438 treatment of Fer-1 (Figure 8, K-M). Additionally, treatment with another ferroptosis inhibitor
439 deferoxamine mesylate (DFOM, a ferric ion depletion reagent) during the DSS
440 administration eliminated the colitis phenotype difference in mice (Supplemental Figure 10,

441 C-K). These data suggest that *Nedd4l* deficiency in IECs promoted the pathogenesis of
442 colitis in a ferroptosis-dependent manner.

443 **Gut microbiota involves in NEDD4L-regulated colitis**

444 The gut microbiota is critical for maintaining gut homeostasis. To further evaluate if the
445 exacerbated colitis in *Nedd4l*-deficient mice compared to control littermates is microbiota-
446 dependent, we co-housed the *Nedd4l*-deficient mice with control littermates for 2 weeks
447 before DSS administration. As shown in Supplemental Figure 11, A-F, co-housing
448 eliminated the development of more severe DSS-induced colitis in *Nedd4l*-deficient mice
449 compared to co-housed control littermates, indicating that NEDD4L protects against colitis
450 in a manner dependent on the gut microbiota. To demonstrate how the microbiota regulates
451 DSS-induced colitis in mice, feces from *Nedd4l^{ff/f}Villin^{Cre}* mice and the control littermates,
452 treated with or without DSS, were collected and then subjected to 16s rDNA sequencing.
453 As shown in Supplemental Figure 11G, the abundance of *Akkermansia* was markedly
454 increased, while the abundances of *Bifidobacterium* and *Lactobacillus* were markedly
455 diminished in *Nedd4l^{ff/f} Villin^{Cre}* mice compared to *Nedd4l^{ff/f}* mice after administration of DSS,
456 with similar abundances in untreated mice. As important commensal intestinal bacteria,
457 *Akkermansia*, *Bifidobacterium*, and *Lactobacillus* play pivotal roles in maintaining intestinal
458 homeostasis(2). However, an abnormally increased abundance of *Akkermansia* could
459 promote the degradation of intestinal mucin, thus exacerbating colitis in mice (42), which
460 is consistent with our phenotype that *Nedd4l^{ff/f} Villin^{Cre}* mice exhibited less intestinal mucin
461 production after DSS treatment visualized by AB-PAS staining of the colon sections
462 (Supplemental Figure 11H). To further investigate the involvement of gut microbiota in

463 NEDD4L-regulated colitis, antimicrobial peptides of the small intestine were detected in
464 untreated and DSS-treated *Nedd4^{fl/fl} Villin^{Cre}* mice and *Nedd4^{fl/fl}* mice. As shown in
465 Supplemental Figure 11, I and J, *Nedd4l* deficiency in mice initially had no effect on the
466 antimicrobial peptide expression without DSS treatment, such as angiogenin, ribonuclease
467 A family, member 4 (*Ang4*), defensin, alpha, 29 (*Defa-rs1*), and defensin, alpha, 20
468 (*Defa20*). DSS treatment resulted in intestinal epithelial cell damages along with decreased
469 antimicrobial peptide gene expression patterns. What's more, *Nedd4l* deficiency in IECs
470 significantly impaired antimicrobial peptide expression in *Nedd4^{fl/fl} Villin^{Cre}* mice than in
471 *Nedd4^{fl/fl}* mice, suggesting a much stronger impact, such as IEC death, plays a critical role
472 during the DSS-induced colitis. Thus, single-housed *Nedd4^{fl/fl} Villin^{Cre}* and *Nedd4^{fl/fl}* mice
473 were gavaged with *Bifidobacterium* and *Lactobacillus* (*Bif&Lac*, 1x10⁸CFU/mice daily)
474 during the induction of colitis. Interestingly, as shown in Supplemental Figure 11, K-N, oral
475 administration of *Bifidobacterium* and *Lactobacillus* significantly restricted colitis
476 development in both *Nedd4^{fl/fl} Villin^{Cre}* mice and *Nedd4^{fl/fl}* mice, characterized by a lower
477 degree of the inflammatory syndrome and stronger mucus secretion ability compared with
478 DSS-treated single-housed *Nedd4^{fl/fl} Villin^{Cre}* mice without bacteria gavage, indicating that
479 the intestinal microbiota involved in NEDD4L-regulated colitis, particularly *Bifidobacterium*
480 and *Lactobacillus*. The IEC samples isolated from the bacteria gavage mice revealed that
481 the administration of microbiota significantly promoted GPX4 and SLC3A2 expression but
482 impaired TFRC expression, thus eliminating the signaling difference between *Nedd4^{fl/fl}*
483 *Villin^{Cre}* and *Nedd4^{fl/fl}* mice (Supplemental Figure 11, O and P), indicating a protective role
484 of gut microbiota in inhibiting ferroptosis through GPX4(43).

485 ***Nedd4l* deficiency promotes the pathogenesis of CAC in mice**

486 AOM/DSS-induced colitis-associated colorectal cancer (CAC) model in mice has been
487 widely used for research on inflammation-related cancer in mice, as mice with more severe
488 inflammation are more likely to develop colorectal cancer (44, 45). Therefore, we further
489 explored the regulatory role of NEDD4L in CAC using *Nedd4l* global deficiency mice and
490 *Nedd4l^{ff}Villin^{Cre}* mice. In vivo, magnetic resonance images (MRI) analysis revealed a
491 marked increase in colon distension of *Nedd4l^{ff}Villin^{Cre}* mice in both axial and coronal
492 images, and a higher number of tumors in the colons of *Nedd4l^{ff}Villin^{Cre}* mice compared to
493 WT mice on day 90 (Figure 9A). As shown in Figure 9, A-D and Supplemental Figure 12,
494 A-C, *Nedd4l*-deficient mice were more susceptible to cancer. Compared to their wild-type
495 littermates, we found higher levels of Ki67⁺ cells per crypt in the adjacent tumor and tumor
496 tissues from *Nedd4l^{+/-}* and *Nedd4l^{ff}Villin^{Cre}* mice following AOM/DSS treatment (Figure 9,
497 E and F and Supplemental Figure 12, D-E), as well as increased lipid peroxidation
498 production in tumor tissues of *Nedd4l^{ff}Villin^{Cre}* mice (Figure 9G). Since NEDD4L regulates
499 the IEC inflammation through ferroptosis signaling, we hypothesized that NEDD4L may
500 regulate CAC through ferroptosis signaling. To test this hypothesis, a ferroptosis inhibitor,
501 DFOM, was *i.p.* injected during DSS treatment as indicated in Figure 9H, to inhibit the
502 inflammatory response. As shown in Figure 9, I-L, DFOM treatment significantly inhibited
503 AOM/DSS-induced tumor formation and lipid peroxidation in *Nedd4l^{ff}Villin^{Cre}* mice
504 compared to the ddH₂O-treated control mice, and further eliminated the phenotype
505 difference between *Nedd4l^{ff}Villin^{Cre}* mice and *Nedd4l^{ff}* mice, suggesting that NEDD4L
506 regulated CAC through ferroptosis signaling.

507 Lipid peroxidation during colitis promotes the pathogenesis of CAC, making colitis a
508 risk factor for colorectal cancer (46–48). Next, we aimed to explore the changes in the
509 NEDD4L gene or protein during CAC. According to the TCGA and GEO data, the *NEDD4L*
510 gene was significantly downregulated in the tumor tissues of patients with colorectal cancer
511 and in the tissues from CAC mice compared to their normal tissues (Supplemental Figure
512 13, A and B). The expression of NEDD4L dynamically changed during the AOM/DSS
513 induction. NEDD4L gene and protein showed no significant changes on the 15th day after
514 the AOM/DSS induction but were slightly downregulated on the 60th day when the mice
515 had minor epithelial hyperplasia/ dysplasia. Moreover, the gene and protein levels of
516 NEDD4L were significantly downregulated on the 90th day after the AOM/DSS induction,
517 when the mice had obvious neoplasia formation (Figure 10, A-C and Supplemental Figure
518 13, C and D). The protein expression of NEDD4L was significantly correlated with both
519 SLC3A2 and GPX4 during the induction of mice CAC (Figure 10 D). NEDD4L expression
520 was significantly inhibited in IECs of adjacent tumor and tumor tissues from CAC mice
521 compared to the distal normal colon (Supplemental Figure 13, E-G). This suggested that
522 the inhibited NEDD4L expression was a consequence of dysregulated intestinal
523 homeostasis, including inflammation damage and tumor formation. Furthermore, NEDD4L
524 expression was negatively correlated with the survival outcomes, and was significantly
525 reduced in advanced tumor stages (Supplemental Figure 13, H-J). Using tissue microarray
526 (TMA)-based IHC of colon sections from patients with colorectal cancer, we found that
527 protein expression of NEDD4L was significantly inhibited in IECs of colonic tumor tissues
528 compared with normal tissues. Meanwhile, lipid peroxidation was significantly enhanced in

529 IECs from tumor and adjacent-tumor tissues compared to the normal tissues (Figure 10, E
530 and F), consistent with the notion that 4-HNE promotes the development of colorectal
531 cancer (46). Moreover, the protein expression of NEDD4L was positively correlated with
532 SLC3A2 and GPX4 in the IECs of patients with colorectal cancer (Figure 11, G and H).
533 Consistently, we found that the gene expression of SLC3A2 was significantly correlated
534 with that of GPX4, but not with NEDD4L, in the GEPIA2 database, suggesting a
535 posttranslational modification of NEDD4L on SLC3A2 (Supplemental Figure 13, K and L).
536 Collectively, our data support the notion that the protective role of NEDD4L in the
537 pathogenesis of AOM/DSS-induced colorectal cancer in mice was dependent on its
538 controlling SLC3A2/GPX4 axis.

539

540

541

542

543

544

545

546

547

548

549

550

551 **Discussion**

552 NEDD4L is a conserved HECT E3 ligase highly expressed in human neurons, the lung,
553 and intestinal systems. It is known to regulate the ubiquitination of membrane proteins (21).
554 Herein, we demonstrated that both the gene and protein levels of NEDD4L were
555 significantly downregulated in IECs from patients with IBDs and colorectal cancer. The
556 expression level of NEDD4L was negatively correlated with the disease status of colitis.
557 Additionally, *Nedd4l* deficiency in mice significantly promoted the pathogenesis of colitis
558 and AOM/DSS-induced tumorigenesis.

559 IEC death is thought to be the main pathological mechanism of dysregulated intestinal
560 homeostasis (13). It has been widely recognized that IEC death induced by apoptosis,
561 necroptosis, and pyroptosis is the first step leading to the destruction of intestinal barrier
562 integrity, thus initiating intestinal mucosa inflammation and resulting in IBDs (1, 3).
563 Therefore, exploring functional proteins involved in maintaining intestinal barrier integrity is
564 of great significance for the early diagnosis and treatment of IBDs. Ferroptosis is a recently
565 defined form of cell death involving lipid peroxidation and iron (Fe). There are some clues
566 that ferroptosis occurs in DSS-induced colitis and IBD and may contribute to their
567 pathogenesis(10, 49, 50). In our study, *Nedd4l*-global deficiency in mice exacerbated DSS-
568 induced colitis compared to the WT mice. Further bone marrow chimera experiments
569 demonstrated that *Nedd4l* deficiency in non-bone marrow cells aggravated DSS-induced
570 colitis, suggesting an important role of NEDD4L in non-bone marrow cells. Goblet cells are
571 the most abundant cells in the intestine and NEDD4L is highly expressed in goblet cells
572 but downregulated in IECs of patients with IBDs, thus we employed the *Nedd4l* IEC knock-

573 out mice to investigate the function of NEDD4L in IECs in colitis. Consistently, *Nedd4l*
574 deficiency in IECs strongly exacerbated DSS/TNBS-induced colitis and AOM/DSS-induced
575 CAC. Further mechanism studies revealed that *Nedd4l* deficiency in IECs induced more
576 severe IEC death and damage of the intestinal barrier through promoting IEC ferroptosis
577 compared with WT mice upon DSS treatment, suggesting that the damaged intestinal
578 barrier integrity served as the initiation factor for NEDD4L to modulate DSS-induced colitis.
579 Intestine is a complex organ composed of many cells, including non-bone marrow-derived
580 cells, such as IECs, mesenchymal cells, endothelial cells, as well as bone marrow-derived
581 cells, including macrophages, monocytes, dendritic cells (DCs), lymphocytes, and even
582 innate lymphoid cells (ILCs), maintaining the intestinal homeostasis through a complex
583 regulatory network. According to scRNA-seq data, *NEDD4L* gene was lowly expressed in
584 bone-marrow-derived and non-bone-marrow-derived cells, thus indicating a potentially
585 limited regulatory function for NEDD4L in these cells.

586 NEDD4L expression was reported to be downregulated in many tumors and psoriasis,
587 suggesting a potential biomarker for diseases (30, 51, 52). In our study, we demonstrated
588 that both the NEDD4L gene and protein were downregulated in IECs of patients with colitis
589 or CAC, and this downregulation was correlated with the disease status of colitis and
590 survival outcomes of colorectal cancer. Our in vitro cellular data indicated that NEDD4L
591 expression was affected by many pathways ending in cell death and TNF- α . However, due
592 to the lack of clinical IBD biopsies from patients with infectious or diverticulitis, we cannot
593 get the conclusion that NEDD4L expression would be inhibited in any inflammatory setting.
594 As colitis develops, intestinal lamina propria infiltrates immune cells secret cytokines,

595 particularly TNF- α , a pivotal mediator of inflammation and cell death, and it is also a key
596 therapeutic target in IBD treatment. As predicted based on our in vitro cell line data, TNF-
597 α may impair the expression of NEDD4L in IECs, further amplifying the inflammatory
598 signaling and enhancing cell death in vivo, resulting in aggravated inflammation and
599 epithelial barrier integrity damage, ultimately leading to IBDs. Thus, NEDD4L may act as a
600 general homeostatic regulator of the epithelial barrier integrity that could be at a common
601 point in many TNF- α -related pathways that converge to mediate cell injury and death.
602 Accumulating evidence suggests that epigenetic modifications, such as chromatin
603 remodeling or DNA methylation, which occur in response to pathological environmental
604 stimuli, contribute to tissue-specific and disease-associated effects mediated by TNF- α (53).
605 Our previous data has demonstrated that NEDD4L expression could be modulated by the
606 IMQ-induced EZH2/H3K27me3 axis in keratinocytes(30). However, it remains to be
607 determined whether the transcriptional regulation of NEDD4L during intestinal injury or cell
608 death is induced by TNF- α -mediated histone methylation, which could be further explored.

609 The ubiquitin-proteasome system (UPS) is a highly finely modulated protein regulation
610 system, which is important for cell proliferation, apoptosis, immunity, and development (54-
611 56), thus regulating inflammatory diseases, tumors, and cardiovascular diseases (54).
612 Based on our unbiased ubiquitinylation MS sequencing, the ferroptosis signaling pathway
613 was substantially enriched in IECs of DSS-treated *Nedd4l*-deficient mice. Our further
614 biochemistry experiment demonstrated that NEDD4L bound to SLC3A2 and promoted the
615 K63-linked ubiquitinylation while inhibiting the K48-linked ubiquitinylation of SLC3A2,
616 positively regulating the protein stability of SLC3A2, thus inhibiting the IEC ferroptosis.

617 Domain mapping data identified that the HECT domain of NEDD4L was required for
618 interaction with and ubiquitinylation of SLC3A2. Our data suggested that SLC3A2 could
619 be the potential target of NEDD4L in IECs, which seems inconsistent with the reported
620 notion that SLC3A2 (CD98) positively regulates intestinal homeostasis by modulating $\alpha 5$ -
621 integrin signaling in IECs (36). However, our in vivo and in vitro data demonstrated that
622 SLC3A2 interacted with GPX4, and its protein expression was positively correlated with
623 that of GPX4, but not with CyclinD1, partly consistent with reported data that SLC3A2 is
624 positively correlated with GPX4(57, 58). Furthermore, ferroptosis-specific inhibitors, Fer-1
625 and DFOM, or a lipid peroxidation scavenger, NAC, eliminated the phenotypic difference
626 of DSS-induced colitis between Nedd4l IEC-deficient mice and WT mice. In contrast, other
627 NEDD4L potential target signaling-related inhibitors, such as BAY 61-3606 and anti-IL17
628 neutralizing antibody, could not eliminate the phenotypic difference of DSS-induced colitis.
629 Collectively, our in vitro and in vivo data suggest that NEDD4L modulated SLC3A2
630 ubiquitinylation to regulate DSS-induced colitis. Further mechanisms need to be explored
631 to clarify the complicated functions of SLC3A2 both in $\alpha 5$ -integrin signaling and
632 ferroptosis signaling.

633 Our study revealed a positive correlation between NEDD4L protein expression and
634 SLC3A2 in humans with IBDs and colorectal cancer, demonstrating that
635 NEDD4L/SLC3A2/GPX4 axis played an important role in colitis and CAC. IL-17R- signaling
636 can affect intestinal epithelial cell homeostasis, differentiation, and tumor development(38-
637 40). However, our data demonstrated that NEDD4L regulated DSS-induced colitis in an IL-
638 17R signaling-independent manner. As colitis is a risk factor, and the AOM/DSS model

639 mice have more severe inflammation, which would drive more serious cancer regardless
640 of any cell-intrinsic effect (44, 45), suggesting that blocking IL-17R- signaling may have no
641 influence on CAC mediated by the *Nedd4l* IEC deficiency. It has been demonstrated that
642 NEDD4 and NEDD4L knockout in IECs regulated the Lgr5 degradation to mediate Wnt
643 signaling and cancer development in APC^{min} mice (27, 60). In addition, a prior study has
644 implicated NEDD4 in mediating Nrf2 to regulate HO-1- and DSS-induced colitis (61, 62).
645 In epithelial cells, E-cadherin suppresses ferroptosis by activating the intracellular NF2
646 (also known as merlin) and Hippo signaling pathway (63). Merlin/NF2, a key activator of
647 the Hippo pathway in growth control and regarded as a key tumor suppressor, is regulated
648 by phosphorylation. However, Merlin ubiquitination is mediated by the E3 ubiquitin ligase
649 NEDD4L, which requires a scaffold protein, AMOTL1, to interact with Merlin (64). Thus,
650 these data suggest a potential role of NEDD4 or NEDD4L in epithelial cell inflammation
651 and cell proliferation-involved colitis or CRC. However, our unbiased ubiquitinylation MS
652 sequencing data and in vivo experiments support that SLC3A2/GPX4-mediated lipid
653 peroxidation production signaling played a dominant role in controlling colitis and CAC.
654 Whether NEDD4L regulates the Lgr5/Wnt signaling or NF2/Yap signaling to control CAC
655 remains to be further studied using their specific inhibitors or genetic knockout mice for the
656 CAC model.

657 The gut microbiota is a key factor of colitis that may directly affect the pathogenesis of
658 colitis (2, 59). In our study, co-housed breeding of *Nedd4l*-deficient and WT mice developed
659 comparable severities of DSS-induced colitis, suggesting that gut microbiota plays a pivotal
660 role in NEDD4L-regulated colitis. Further analysis, including 16S rDNA-sequencing of the

661 feces and in vivo supplement of commensal intestinal bacteria, revealed that the
662 *Lactobacillus* and *Bifidobacterium* were critical for NEDD4L-regulated colitis. Our signaling
663 study demonstrated that supplementation of *Lactobacillus* and *Bifidobacterium* blocked the
664 GPX4-mediated ferroptosis signaling, suggesting an important role of these gut microbiota
665 in ferroptosis-mediated colitis.

666 In conclusion, our study demonstrated a significant reduction in the expression of the
667 E3 ubiquitin ligase NEDD4L in IECs of patients with IBDs and colorectal cancer. Additionally,
668 *Nedd4l* knockout in mice significantly enhanced DSS/TNBS-induced colitis and AOM/DSS-
669 induced CAC by triggering SLC3A2-mediated ferroptosis (Graphical abstract). This study
670 provides a potential diagnostic biomarker and clinical treatment target for inflammatory
671 bowel diseases and CAC.

672

673

674

675

676

677

678

679

680

681

682

683 **Methods**

684 **Sex as a biological variable**

685 Our study utilized both male and female biopsies from humans and mice for the study, as
686 sex was not considered a biological variable.

687 **Animals**

688 Heterozygous *Nedd4l* mice (on a BALB/cByJ background) were purchased from
689 JAX[®] Mice, America. *NEDD4L^{ff}* mice (on a C57BL/6J background) were purchased from
690 Cyagen Bioscience. Knockout (KO) mice and the *WT* littermate control mice were
691 generated by crossing *Nedd4l* heterozygous. *Nedd4l* IEC-knockout mice were generated
692 by crossing *Nedd4l^{ff}* mice with *Villin^{Cre}* mice (on a C57BL/6J background). All mice were
693 maintained under the specific-pathogen-free (SPF) condition in the Laboratory Animal
694 Center of Zhejiang University. Eight- to ten-week-old mice were studied using TNBS or
695 DSS-induced colitis models as described previously(65). For inhibition experiments in vivo,
696 the *Nedd4l^{ff} Villin^{Cre}* and corresponding control mice were daily treated with Fer1
697 (5 μmol/kg), DFOM (200mg/kg), NCA (300mg/kg), BAY 61-3066 (5 mg/kg), anti-IL17A
698 antibody (100 μg/mouse), or corresponding control vehicle respectively, 3 days before 2%
699 DSS administration until to the end of experiments.

700 **Statistical analysis**

701 The statistical analysis was performed using a log-rank test for survival two curves analysis,
702 a two-way ANOVA test for two curves analysis, a Pearson correlation test for correlation
703 analysis, or a 2-tailed unpaired Student's t-test for two groups analysis. When appropriate,
704 the statistical significance of differences among multiple groups was analyzed using one-

705 way ANOVA with the Bonferroni correction. Differences were considered significant at
706 $p < 0.05$.

707 **Study approval**

708 Written patient consent was provided, and ethics approval for human samples was granted
709 by the Medical Ethics Committee of Zhejiang University School of Medicine (ethics
710 approval 2021-005, 20210125-30, IIT20240689BR) for harvesting human tissues. All
711 animal research was performed under a protocol approved by the Medical Experimental
712 Animal Care Commission of Zhejiang University (ethics approval 202118445,
713 ZJU20240729).

714 **Disclosure and Competing Interests Statement**

715 The authors declare that they have no conflict of interest.

716 **Data availability**

717 Raw data of **protein** sequencing were deposited in iProX
718 (<https://www.iprox.cn/page/home.html>) under accession no. PXD057172 and PXD057173.

719 **Raw data of RNA sequencing were deposited in GEO under accession no. GSE282883**
720 **and GSE282497.** The values for all data points in the graphs are reported in the Supporting

721 Data Values file. Additional methods are provided in the Supplemental material.

722 **Author Contributions**

723 J.L., W.L., N.W., Y.Y., H, W., X. A., H.LI., H.LUI., Y.J., and Y.W. performed experiments. J.L.,
724 W.L., and Y.J. performed the statistical analysis. X.C. and J.X. provided single cell analysis.
725 X.L, J.L, and Z.X. provided some reagents. T.Z., X.W., and W.L. designed the study. J.L.
726 and W.L. drafted the manuscript.

727 **Acknowledgments**

728 This work is supported by grants from the National Natural Science Foundation of China
729 (82071774, 82171765, 81901595, 82371763), Zhejiang Province Natural Science
730 Foundation project (LZ22H100001, LY22H100002), and the Science and Technology
731 Bureau of Hangzhou, Zhejiang Province (20212013B05 to J.P. (Jianping Pan)). We thank
732 Chun Guo, Jiajia Wang, Jingyao Chen, Shuangshuang Liu, and Yanwei Li from the Core
733 Facilities, Zhejiang University School of Medicine for their technical support.

734

735

736

737

738

739

740

741

742

743

744

745

746

747

748

749

750 **References**

- 751 1. Peterson LW, and Artis D. Intestinal epithelial cells: regulators of barrier function and immune
752 homeostasis. *Nat Rev Immunol.* 2014;14(3):141-53.
- 753 2. Thaïss CA, Zmora N, Levy M, and Elinav E. The microbiome and innate immunity. *Nature.*
754 2016;535(7610):65-74.
- 755 3. Turner JR. Intestinal mucosal barrier function in health and disease. *Nat Rev Immunol.*
756 2009;9(11):799-809.
- 757 4. Parikh K, Antanaviciute A, Fawcner-Corbett D, Jagielowicz M, Aulicino A, Lagerholm C, et al.
758 Colonic epithelial cell diversity in health and inflammatory bowel disease. *Nature.*
759 2019;567(7746):49-55.
- 760 5. Jiang X, Stockwell BR, and Conrad M. Ferroptosis: mechanisms, biology and role in disease. *Nat*
761 *Rev Mol Cell Biol.* 2021;22(4):266-82.
- 762 6. Wang W, Green M, Choi JE, Gijon M, Kennedy PD, Johnson JK, et al. CD8(+) T cells regulate
763 tumour ferroptosis during cancer immunotherapy. *Nature.* 2019;569(7755):270-4.
- 764 7. Liang D, Minikes AM, and Jiang X. Ferroptosis at the intersection of lipid metabolism and
765 cellular signaling. *Mol Cell.* 2022;82(12):2215-27.
- 766 8. Chen X, Kang R, Kroemer G, and Tang D. Broadening horizons: the role of ferroptosis in cancer.
767 *Nat Rev Clin Oncol.* 2021;18(5):280-96.
- 768 9. Panda SK, Peng V, Sudan R, Ulezko Antonova A, Di Luccia B, Ohara TE, et al. Repression of the
769 aryl-hydrocarbon receptor prevents oxidative stress and ferroptosis of intestinal intraepithelial
770 lymphocytes. *Immunity.* 2023.
- 771 10. Xu M, Tao J, Yang Y, Tan S, Liu H, Jiang J, et al. Ferroptosis involves in intestinal epithelial cell

- 772 death in ulcerative colitis. *Cell Death Dis.* 2020;11(2):86.
- 773 11. Koppula P, Zhuang L, and Gan B. Cystine transporter SLC7A11/xCT in cancer: ferroptosis,
774 nutrient dependency, and cancer therapy. *Protein Cell.* 2021;12(8):599-620.
- 775 12. Bulek K, Zhao J, Liao Y, Rana N, Corridoni D, Antanaviciute A, et al. Epithelial-derived gasdermin
776 D mediates nonlytic IL-1beta release during experimental colitis. *J Clin Invest.*
777 2020;130(8):4218-34.
- 778 13. Patankar JV, and Becker C. Cell death in the gut epithelium and implications for chronic
779 inflammation. *Nat Rev Gastroenterol Hepatol.* 2020;17(9):543-56.
- 780 14. Bertrand MJ, Doiron K, Labbe K, Korneluk RG, Barker PA, and Saleh M. Cellular inhibitors of
781 apoptosis cIAP1 and cIAP2 are required for innate immunity signaling by the pattern
782 recognition receptors NOD1 and NOD2. *Immunity.* 2009;30(6):789-801.
- 783 15. Song H, Liu B, Huai W, Yu Z, Wang W, Zhao J, et al. The E3 ubiquitin ligase TRIM31 attenuates
784 NLRP3 inflammasome activation by promoting proteasomal degradation of NLRP3. *Nat*
785 *Commun.* 2016;7:13727.
- 786 16. Vereecke L, Vieira-Silva S, Billiet T, van Es JH, Mc Guire C, Slowicka K, et al. A20 controls
787 intestinal homeostasis through cell-specific activities. *Nat Commun.* 2014;5:5103.
- 788 17. Zhang H, Cui Z, Cheng D, Du Y, Guo X, Gao R, et al. RNF186 regulates EFNB1 (ephrin B1)-EPHB2-
789 induced autophagy in the colonic epithelial cells for the maintenance of intestinal homeostasis.
790 *Autophagy.* 2021;17(10):3030-47.
- 791 18. Vereecke L, Sze M, Mc Guire C, Rogiers B, Chu Y, Schmidt-Supprian M, et al. Enterocyte-specific
792 A20 deficiency sensitizes to tumor necrosis factor-induced toxicity and experimental colitis. *J*
793 *Exp Med.* 2010;207(7):1513-23.

- 794 19. Lin H, Feng L, Cui KS, Zeng LW, Gao D, Zhang LX, et al. The membrane-associated E3 ubiquitin
795 ligase MARCH3 downregulates the IL-6 receptor and suppresses colitis-associated
796 carcinogenesis. *Cell Mol Immunol*. 2021;18(12):2648-59.
- 797 20. Zou M, Zeng QS, Nie J, Yang JH, Luo ZY, and Gan HT. The Role of E3 Ubiquitin Ligases and
798 Deubiquitinases in Inflammatory Bowel Disease: Friend or Foe? *Front Immunol*.
799 2021;12:769167.
- 800 21. Manning JA, and Kumar S. Physiological Functions of Nedd4-2: Lessons from Knockout Mouse
801 Models. *Trends Biochem Sci*. 2018;43(8):635-47.
- 802 22. Goel P, Manning JA, and Kumar S. NEDD4-2 (NEDD4L): the ubiquitin ligase for multiple
803 membrane proteins. *Gene*. 2015;557(1):1-10.
- 804 23. Verrey F, Fakitsas P, Adam G, and Staub O. Early transcriptional control of ENaC
805 (de)ubiquitylation by aldosterone. *Kidney Int*. 2008;73(6):691-6.
- 806 24. Duerr J, Leitz DHW, Szczygiel M, Dvornikov D, Fraumann SG, Kreutz C, et al. Conditional deletion
807 of Nedd4-2 in lung epithelial cells causes progressive pulmonary fibrosis in adult mice. *Nat*
808 *Commun*. 2020;11(1):2012.
- 809 25. Henshall TL, Manning JA, Alfassy OS, Goel P, Boase NA, Kawabe H, et al. Deletion of Nedd4-2
810 results in progressive kidney disease in mice. *Cell Death Differ*. 2017;24(12):2150-60.
- 811 26. Gao S, Alarcon C, Sapkota G, Rahman S, Chen PY, Goerner N, et al. Ubiquitin ligase Nedd4L
812 targets activated Smad2/3 to limit TGF-beta signaling. *Mol Cell*. 2009;36(3):457-68.
- 813 27. Novellademunt L, Kucharska A, Jamieson C, Prange-Barczynska M, Baulies A, Antas P, et al.
814 NEDD4 and NEDD4L regulate Wnt signalling and intestinal stem cell priming by degrading LGR5
815 receptor. *EMBO J*. 2020;39(3):e102771.

- 816 28. Gao P, Ma X, Yuan M, Yi Y, Liu G, Wen M, et al. E3 ligase Nedd4l promotes antiviral innate
817 immunity by catalyzing K29-linked cysteine ubiquitination of TRAF3. *Nat Commun.*
818 2021;12(1):1194.
- 819 29. Li H, Wang N, Jiang Y, Wang H, Xin Z, An H, et al. E3 ubiquitin ligase NEDD4L negatively regulates
820 inflammation by promoting ubiquitination of MEKK2. *EMBO Rep.* 2022;23(11):e54603.
- 821 30. Liu H, Lin W, Liu Z, Song Y, Cheng H, An H, et al. E3 ubiquitin ligase NEDD4L negatively regulates
822 keratinocyte hyperplasia by promoting GP130 degradation. *EMBO Rep.* 2021;22(5):e52063.
- 823 31. Jiang C, Kawabe H, and Rotin D. The Ubiquitin Ligase Nedd4L Regulates the Na/K/2Cl Co-
824 transporter NKCC1/SLC12A2 in the Colon. *J Biol Chem.* 2017;292(8):3137-45.
- 825 32. Luo G, He Y, Yang F, Zhai Z, Han J, Xu W, et al. Blocking GSDME-mediated pyroptosis in renal
826 tubular epithelial cells alleviates disease activity in lupus mice. *Cell Death Discov.* 2022;8(1):113.
- 827 33. Tigano M, Vargas DC, Tremblay-Belzile S, Fu Y, and Sfeir A. Nuclear sensing of breaks in
828 mitochondrial DNA enhances immune surveillance. *Nature.* 2021;591(7850):477-81.
- 829 34. Wang Y, Gao W, Shi X, Ding J, Liu W, He H, et al. Chemotherapy drugs induce pyroptosis through
830 caspase-3 cleavage of a gasdermin. *Nature.* 2017;547(7661):99-103.
- 831 35. Xu D, Jin T, Zhu H, Chen H, Ofengeim D, Zou C, et al. TBK1 Suppresses RIPK1-Driven Apoptosis
832 and Inflammation during Development and in Aging. *Cell.* 2018;174(6):1477-91 e19.
- 833 36. Nguyen HT, Dalmasso G, Torkvist L, Halfvarson J, Yan Y, Laroui H, et al. CD98 expression
834 modulates intestinal homeostasis, inflammation, and colitis-associated cancer in mice. *J Clin*
835 *Invest.* 2011;121(5):1733-47.
- 836 37. Maspero E, Valentini E, Mari S, Cecatiello V, Soffientini P, Pasqualato S, et al. Structure of a
837 ubiquitin-loaded HECT ligase reveals the molecular basis for catalytic priming. *Nat Struct Mol*

- 838 *Biol.* 2013;20(6):696-701.
- 839 38. Brabec T, Voboril M, Schierova D, Valter E, Splichalova I, Dobes J, et al. IL-17-driven induction
840 of Paneth cell antimicrobial functions protects the host from microbiota dysbiosis and
841 inflammation in the ileum. *Mucosal Immunol.* 2023;16(4):373-85.
- 842 39. Chandra V, Li L, Le Roux O, Zhang Y, Howell RM, Rupani DN, et al. Gut epithelial Interleukin-17
843 receptor A signaling can modulate distant tumors growth through microbial regulation. *Cancer*
844 *Cell.* 2024;42(1):85-100 e6.
- 845 40. Wang K, Kim MK, Di Caro G, Wong J, Shalapour S, Wan J, et al. Interleukin-17 receptor a
846 signaling in transformed enterocytes promotes early colorectal tumorigenesis. *Immunity.*
847 2014;41(6):1052-63.
- 848 41. Yip KH, Kolesnikoff N, Hauschild N, Biggs L, Lopez AF, Galli SJ, et al. The Nedd4-2/Ndfip1 axis is
849 a negative regulator of IgE-mediated mast cell activation. *Nat Commun.* 2016;7:13198.
- 850 42. Desai MS, Seekatz AM, Koropatkin NM, Kamada N, Hickey CA, Wolter M, et al. A Dietary Fiber-
851 Deprived Gut Microbiota Degrades the Colonic Mucus Barrier and Enhances Pathogen
852 Susceptibility. *Cell.* 2016;167(5):1339-53 e21.
- 853 43. Deng F, Zhao BC, Yang X, Lin ZB, Sun QS, Wang YF, et al. The gut microbiota metabolite capsiate
854 promotes Gpx4 expression by activating TRPV1 to inhibit intestinal ischemia reperfusion-
855 induced ferroptosis. *Gut Microbes.* 2021;13(1):1-21.
- 856 44. Tanaka T, Kohno H, Suzuki R, Yamada Y, Sugie S, and Mori H. A novel inflammation-related
857 mouse colon carcinogenesis model induced by azoxymethane and dextran sodium sulfate.
858 *Cancer Sci.* 2003;94(11):965-73.
- 859 45. Zaki MH, Vogel P, Malireddi RK, Body-Malapel M, Anand PK, Bertin J, et al. The NOD-like

860 receptor NLRP12 attenuates colon inflammation and tumorigenesis. *Cancer Cell*.
861 2011;20(5):649-60.

862 46. Yang Y, Huycke MM, Herman TS, and Wang X. Glutathione S-transferase alpha 4 induction by
863 activator protein 1 in colorectal cancer. *Oncogene*. 2016;35(44):5795-806.

864 47. Wang X, Yang Y, and Huycke MM. Commensal bacteria drive endogenous transformation and
865 tumour stem cell marker expression through a bystander effect. *Gut*. 2015;64(3):459-68.

866 48. Gobert AP, Boutaud O, Asim M, Zagol-Ikapitte IA, Delgado AG, Latour YL, et al. Dicarbonyl
867 Electrophiles Mediate Inflammation-Induced Gastrointestinal Carcinogenesis.
868 *Gastroenterology*. 2021;160(4):1256-68 e9.

869 49. Chen Y, Zhang P, Chen W, and Chen G. Ferroptosis mediated DSS-induced ulcerative colitis
870 associated with Nrf2/HO-1 signaling pathway. *Immunol Lett*. 2020;225:9-15.

871 50. Wang S, Liu W, Wang J, and Bai X. Curculigoside inhibits ferroptosis in ulcerative colitis through
872 the induction of GPX4. *Life Sci*. 2020;259:118356.

873 51. Guarnieri AL, Towers CG, Drasin DJ, Oliphant MUJ, Andrysiak Z, Hotz TJ, et al. The miR-106b-25
874 cluster mediates breast tumor initiation through activation of NOTCH1 via direct repression of
875 NEDD4L. *Oncogene*. 2018;37(28):3879-93.

876 52. Li G, Song Z, Wu C, Li X, Zhao L, Tong B, et al. Downregulation of NEDD4L by EGFR signaling
877 promotes the development of lung adenocarcinoma. *J Transl Med*. 2022;20(1):47.

878 53. Kalliolias GD, and Ivashkiv LB. TNF biology, pathogenic mechanisms and emerging therapeutic
879 strategies. *Nat Rev Rheumatol*. 2016;12(1):49-62.

880 54. Popovic D, Vucic D, and Dikic I. Ubiquitination in disease pathogenesis and treatment. *Nat Med*.
881 2014;20(11):1242-53.

- 882 55. Cockram PE, Kist M, Prakash S, Chen SH, Wertz IE, and Vucic D. Ubiquitination in the regulation
883 of inflammatory cell death and cancer. *Cell Death Differ.* 2021;28(2):591-605.
- 884 56. Liu J, Qian C, and Cao X. Post-Translational Modification Control of Innate Immunity. *Immunity.*
885 2016;45(1):15-30.
- 886 57. Fiore A, Zeitler L, Russier M, Gross A, Hiller MK, Parker JL, et al. Kynurenine importation by
887 SLC7A11 propagates anti-ferroptotic signaling. *Mol Cell.* 2022;82(5):920-32 e7.
- 888 58. Cao T, Zhou J, Liu Q, Mao T, Chen B, Wu Q, et al. Interferon-gamma induces salivary gland
889 epithelial cell ferroptosis in Sjogren's syndrome via JAK/STAT1-mediated inhibition of system
890 Xc(). *Free Radic Biol Med.* 2023;205:116-28.
- 891 59. Brennan CA, and Garrett WS. Gut Microbiota, Inflammation, and Colorectal Cancer. *Annu Rev*
892 *Microbiol.* 2016;70:395-411.
- 893 60. Lu C, Thoeni C, Connor A, Kawabe H, Gallinger S, and Rotin D. Intestinal knockout of Nedd4
894 enhances growth of Apc(min) tumors. *Oncogene.* 2016;35(45):5839-49.
- 895 61. Chuang HY, Hsu LY, Pan CM, Pikatan NW, Yadav VK, Fong IH, et al. The E3 Ubiquitin Ligase
896 NEDD4-1 Mediates Temozolomide-Resistant Glioblastoma through PTEN Attenuation and
897 Redox Imbalance in Nrf2-HO-1 Axis. *Int J Mol Sci.* 2021;22(19).
- 898 62. Hong Z, Cao J, Liu D, Liu M, Chen M, Zeng F, et al. Celastrol targeting Nedd4 reduces Nrf2-
899 mediated oxidative stress in astrocytes after ischemic stroke. *J Pharm Anal.* 2023;13(2):156-69.
- 900 63. Wu J, Minikes AM, Gao M, Bian H, Li Y, Stockwell BR, et al. Intercellular interaction dictates
901 cancer cell ferroptosis via NF2-YAP signalling. *Nature.* 2019;572(7769):402-6.
- 902 64. Wei Y, Yee PP, Liu Z, Zhang L, Guo H, Zheng H, et al. NEDD4L-mediated Merlin ubiquitination
903 facilitates Hippo pathway activation. *EMBO Rep.* 2020;21(12):e50642.

904 65. Lin W, Ma C, Su F, Jiang Y, Lai R, Zhang T, et al. Raf kinase inhibitor protein mediates intestinal
905 epithelial cell apoptosis and promotes IBDs in humans and mice. *Gut*. 2017;66(4):597-610.

906

907

908

909

910

911

912

913

914

915

916

917

918

919

920

921

922

923

924

925

926 **Figure legends**

927 **Figure 1. NEDD4L Expression is significantly down-regulated in intestinal epithelial**
928 **cells (IECs) of patients with IBDs.**

929 **(A, B)** Statistical analysis of NEDD4L immunohistochemical (IHC) intensity in the biopsies
930 from Xijing Hospital (cohort1) **(A)** and representative IHC staining of sections traced with
931 anti-NEDD4L antibody **(B)**. Normal control (HC) n=40 and UC n=83. Scale bar, 50 μ m. **(C,**
932 **D)** Statistical analysis of NEDD4L IHC intensity in the biopsies from the First Affiliated
933 Hospital of Zhejiang University, School of Medicine (FAHZU, cohort2) **(C)** and
934 representative IHC staining of sections **(D)**. Normal control (HC) n=31, UC n=36, and CD
935 n=41. Scale bar, 50 μ m. **(E, F)** Statistical analysis of NEDD4L IHC intensity in the biopsies
936 with disease status record from cohort 2 and representative IHC staining of sections traced
937 with anti-NEDD4L antibody**(F)**. Mild n=14 and Moderate/Severe n=48. Scale bar, 50 μ m.
938 **(G, H)** qPCR analysis **(G)** and representative western blotting of NEDD4L in the mucosa
939 from patients with IBDs and their corresponding normal tissues (n=24/group). **(I, J)**
940 Western blotting analysis **(I)** and protein intensity analysis **(J)** according to **(I)** using ImageJ
941 software of NEDD4L from the IECs of the wild-type (WT) mice treated without or with DSS
942 for 4 days (n=5/group). Red arrows indicated NEDD4L expression in IECs, and green
943 arrows indicated NEDD4L expression in non-IECs.

944 Data represent mean \pm SEM. Each dot means independent samples. ns, no significant
945 difference. ****, P<0.0001; ***, P<0.001; **, P<0.01. Statistical analysis was performed
946 using 1-way ANOVA multiple comparisons in **C**, and a 2-tailed Student's t-test in **A, E, G,**
947 and **J**.

948 **Figure 2. *Nedd4l* deficiency in mice promotes dextran sulfate sodium (DSS)-induced**
949 **experimental colitis in a non-hematopoietic cell-dependent manner.**

950 **(A)** *Nedd4l* global-deficient mice (*Nedd4l*^{-/-}) and control littermates (*Nedd4l*^{+/+}) were
951 administered with 4 % DSS for 5 days followed by water to induce acute colitis. Mouse
952 death was monitored until day 9. n=20/group. **(B-D)** *Nedd4l*^{-/-} mice and *Nedd4l*^{+/+} were
953 administered with 3 % DSS for 5 days followed by water until day 9. n=9/group. **(B)**Body
954 weight change, **(C)** bleeding scores, **(D)** colon length, **(E)** gross morphology images, and

955 **(F)** H&E staining of the colons from *Nedd41^{+/+}* and *Nedd41^{+/-}* mice. Red arrows point to
956 epithelial degeneration and green arrows to inflammatory infiltrates. Scale bar, 200 μ m or
957 50 μ m (amplified sections). **(G–J)** The bone marrow from *Nedd41^{+/+}*(WT) and *Nedd41^{-/-}*
958 (KO) mice were transferred to WT (n=7) and KO(n=10) mice to generate bone marrow
959 reconstitution mice. The bone marrow reconstitution mice were subjected to 3% DSS
960 treatment for 5 days followed by water, and **(G)** mouse death and **(H)** body weight changes
961 were monitored until day 9. **(I, J)** In a separate experiment, **(I)** colon length and **(J)** gross
962 morphology images of the colons from mice on day 6 after DSS treatment. n=4/group. Red
963 arrows point to epithelial degeneration and green arrows to inflammatory infiltrates.
964 Data represent mean \pm SEM from at least two independent experiments. Each dot means
965 independent samples. ns, no significant difference. ****, P<0.0001; ***, P<0.001; **, P<0.01.
966 Statistical analysis was performed using a log-rank test in **A** and **G**, a two-way ANOVA test
967 in **B, C**, and **H**, and a 2-tailed Student's t-test in **D** and **I**.

968 **Figure 3. *Nedd41* deficiency in IECs promotes DSS-induced colitis in mice.**

969 **(A)** *Nedd41* IEC-deficient mice (*Nedd41^{ff/f}Villin^{Cre}*, n=8) and control littermates (*Nedd41^{ff/f}*, n=7)
970 were administered with 2.5 % DSS for 5 days followed by water to induce acute colitis.
971 Mouse death was monitored until day 12. **(B–F)** In a separate experiment, *Nedd41^{ff/f}Villin^{Cre}*
972 (n=7) mice and control *Nedd41^{ff/f}* (n=8) mice were administered with 2% DSS for 5 days
973 followed by water until day 9 to induce colitis. **(B)** Body weight change, **(C)** bleeding scores,
974 **(D)** colon length, **(E)** gross morphology images, and **(F)** H&E staining of the colons from
975 *Nedd41^{ff/f}Villin^{Cre}* and *Nedd41^{ff/f}* mice. Red arrows point to epithelial degeneration and green
976 arrows to inflammatory infiltrates. Scale bar, 200 μ m or 50 μ m (amplified sections). **(G, H)**
977 Colon-infiltrated immune cells of *Nedd41^{ff/f}Villin^{Cre}* and *Nedd41^{ff/f}* mice from **(B)** were analyzed
978 by flow cytometer analysis (n = 3–4/group). Red arrows point to epithelial degeneration
979 and green arrows to inflammatory infiltrates.
980 Data represent mean \pm SEM from at least two independent experiments. Each dot means
981 independent samples. ns, no significant difference. ***, P<0.001; **, P<0.01; *, P<0.05.
982 Statistical analysis was performed using a log-rank test in **A**, a two-way ANOVA test in **B**
983 and **C**, and a 2-tailed Student's t-test in **D, G**, and **H**.

984 **Figure 4. *Nedd4l* deficiency in IECs promotes IEC ferroptosis, resulting in barrier**
985 **integrity damage.**

986 **(A)** KEGG analysis of colonic tissues on the 7th day from the *Nedd4l^{ff}Villin^{Cre}* and *Nedd4l^{ff}*
987 mice administered 2 % DSS. **(B)** The indicated mice were treated as in **(A)** and were orally
988 fed with FITC-dextran (500 mg/kg) for 4 h before sacrifice. The serum levels of FITC-
989 dextran were detected by measuring the mean fluorescence intensity (MFI) of FITC-
990 dextran. **(C)** In a separate experiment, the indicated mice were treated as in **(A)**, and colon
991 tissues were further subjected to ZO-1 immunofluorescence (IF) staining. Red IF indicated
992 ZO-1 and blue (DAPI) indicated nucleic. Scale bars, 50 μ m. **(D)** KEGG analysis of
993 ubiquitylation mass spectrometry from IECs of the indicated mice treated as in **(A)**. **(E-H)**
994 Colon tissues from DSS-treated *Nedd4l^{ff}Villin^{Cre}* and *Nedd4l^{ff}* mice were subjected to
995 TUNEL **(E, F)** and 4-HNE **(G, H)** IHC staining. The TUNEL **(F)** and 4-HNE **(H)** IHC staining
996 were scored and analyzed. Scale bars, 50 μ m. **(I)** In a separate experiment, the IECs from
997 DSS-treated *Nedd4l^{ff}Villin^{Cre}* and *Nedd4l^{ff}* mice were subjected to MDA analysis. **(J)**
998 Representative transmission electron microscope (TEM) images from colonic tissue
999 sections of DSS-treated *Nedd4l^{ff}Villin^{Cre}* and *Nedd4l^{ff}* mice. Scale bars, 2 μ m or 0.5 μ m
1000 (amplified sections). **(K, L)** Representative microscope images **(K)** and flow cytometer
1001 analysis **(L)** of small intestinal organoids isolated and cultured from crypts of
1002 *Nedd4l^{ff}Villin^{Cre}* and *Nedd4l^{ff}* mice treated with DMSO(Control), DSS (0.5% w/v),
1003 Erastin(30 μ M), Erastin2 (30 μ M), and RSL3 (5 μ M) for 24hr, followed by DAPI and BODIPY
1004 C11 staining. n = 3/group. Scale bars, 100 μ m.

1005 Data represent mean \pm SEM from at least two independent experiments. Each dot means
1006 independent samples. ns, no significant difference. *P<0.05, **P<0.01. Statistical analysis
1007 was performed using a 2-tailed Student's t-test in **B, E, H, I, and L**.

1008 **Figure 5. NEDD4L positively regulates SLC3A2 expression.**

1009 **(A)** Volcano plots of protein abundance fold change based on ubiquitylation mass
1010 spectrometry of **Figure 4D**. **(B)** Venn analysis showed the potential targets of NEDD4L
1011 based on interaction MS analysis in Flag-tagged NEDD4L stable expressed HCT116 cells
1012 and ubiquitylation MS analysis. The list showed the overlapped targets of NEDD4L in **(A)**

1013 and **(B)**. **(C)** Representative IHC staining of SLC3A2 from *Nedd4^{fl/fl}Villin^{Cre}* and *Nedd4^{fl/fl}*
1014 mice treated with DSS on day 5. Scale bar, 100 μ m or 50 μ m (amplified sections). **(D, E)**
1015 Western blotting analysis **(D)** and statistical analysis **(E)** of the indicated protein intensity
1016 in the IECs from *Nedd4^{fl/fl}Villin^{Cre}* (n =7) and *Nedd4^{fl/fl}* (n =4) mice treated as **Figure 3B**. **(F,**
1017 **G)** Representative IHC staining **(F)** and correlative analysis **(G)** of SLC3A2 and NEDD4L
1018 from colonic sections from CD patients (n=13). Scale bars, 50 μ m. **(H)** Immunoblot analysis
1019 of the indicated proteins in small intestinal organoids isolated and cultured from crypts of
1020 *Nedd4^{fl/fl}Villin^{Cre}* and *Nedd4^{fl/fl}* mice, with 0.5% DSS treatment for the indicated time. **(I, J)**
1021 *NEDD4L* knockout (sg*NEDD4L*) and negative control (sg*NTC*) HCT116 cell lines, or Myc-
1022 tagged NEDD4L, Myc-tagged NEDD4L-C942A (Myc-NEDD4L-CA), or Myc-tagged null
1023 control plasmids (Ctrl) transfected HCT116 cells were treated with 2% DSS for the
1024 indicated time and then subjected to immunoblot analysis of the indicated proteins. **(K-M)**
1025 Immunoblot analysis of the indicated proteins in HCT116 cells **(K)**, SW480 cells **(L)**, and
1026 RKO cells **(M)** transfected with the siRNA targeted to NEDD4L (si*NEDD4L*) or negative
1027 control (si*NC*) and treated as in **(I)**.
1028 Data represent mean \pm SEM from at least two independent experiments. Each dot means
1029 independent samples. ns, no significant difference. ***, P<0.001; **, P<0.01; *, P<0.05.
1030 Statistical analysis was performed using a 2-tailed Student's t-test in **E**, and a Pearson
1031 correlation test in **G**.

1032 **Figure 6. SLC3A2 negatively regulates ferroptosis.**

1033 **(A-C)** The multitype cell lines, including HCT116 cells **(A)**, SW480 cells **(B)**, and RKO cells
1034 **(C)** were transfected with the siRNA targeted to *SLC3A2* (si*SLC3A2*) or negative control
1035 (si*NC*). The cells were treated with 2% DSS for the indicated time and then subjected to
1036 CCK8 assay. **(D-F)** The multitype cell lines were treated as in **(A-C)** with or without Fer-
1037 1(2 μ M) treatment. The cells were then subjected to flow cytometer analysis of BODIPY
1038 C11 staining to measure lipid peroxidation production. **(G-I)** The multitype cell lines were
1039 treated as in **(A-C)** for the indicated time and then subjected to immunoblot analysis of the
1040 indicated proteins. **(J-M)** HCT116 cells were overexpressed with Flag-tagged SLC3A2 or
1041 Flag-tagged null control plasmids. The cells were treated with 2% DSS or indicated

1042 inducers for the stated time, and then subjected to CCK8 assay **(J)**, MDA assay**(K)**, flow
1043 cytometer analysis of BODIPY C11 staining **(L)**, and immunoblot analysis of immunoblot
1044 analysis of the indicated proteins **(M)**. **(N-P)** HCT116 cells were transfected with siRNA
1045 negative control (siNC) or NEDD4L (siNEDD4L) specific oligo and then overexpressed with
1046 Flag-tagged SLC3A2 or Flag-tagged null control plasmid. The cells were treated with 2%
1047 DSS for the indicated time and then subjected to CCK8 assay**(N)** and lipid peroxidation
1048 **(O)**. Immunoblot analysis of the indicated proteins **(P)**.

1049 Data represent mean \pm SEM from at least two independent experiments. Each dot means
1050 independent samples. ns, no significant difference. ***, $P < 0.001$; **, $P < 0.01$; *, $P < 0.05$.
1051 Statistical analysis was performed using a 2-tailed Student's t-test in **A-F, J-K, N, and O**.

1052 **Figure 7. NEDD4L ubiquitinates SLC3A2.**

1053 **(A)** Immunoblot analysis of NEDD4L and SLC3A2 co-immunoprecipitated with anti-
1054 SLC3A2 antibody from lysates of HCT116 cells treated with 2%DSS for the indicated time.

1055 **(B, C)** Immunoblot analysis of Myc-tagged proteins and Flag-tagged SLC3A2 co-
1056 immunoprecipitated with anti-Myc antibody from lysates of HEK293T cells co-transfected
1057 with indicated plasmids. **(D)** Immunoblot analysis of NEDD4L, SLC3A2, and Ub, which
1058 were co-immunoprecipitated with anti-Ub antibody from lysates of NEDD4L (sgNEDD4L)
1059 or negative control (sgNTC) knockout HCT116 cells treated with 2%DSS for the indicated
1060 time. **(E)** Immunoblot analysis of total ubiquitination of Flag-tagged SLC3A2 following co-

1061 immunoprecipitated of Flag-tagged with anti-Flag antibody from lysates of HEK293T cells
1062 co-transfected with indicated plasmids. **(F)** Immunoblot analysis of Ub-linked flag-tagged
1063 EGFP or SLC3A2 incubated with Myc-tagged NEDD4L, Myc-tagged NEDD4L-C942A (CA),
1064 or Myc-tagged EGFP recombinant protein in the present of the full complement of
1065 ubiquitination reaction components, including E1, E2, Ub, and ATP in vitro. **(G, H)**

1066 Immunoblot analysis of ubiquitination of Flag-tagged SLC3A2 following co-
1067 immunoprecipitated of SLC3A2 with anti-Flag antibody from lysates of HEK293T cells co-
1068 transfected with indicated plasmids. **(I)** Immunoblot analysis of K63Ub, K48Ub, Ub, GPX4,
1069 TFRC, SLC3A2, NEDD4L, and actin, which was co-immunoprecipitated with anti-SLC3A2
1070 antibody from lysates of NEDD4L (sgNEDD4L) or negative control (sgNTC) knockout

1071 HCT116 cells treated with 2%DSS for the indicated time pre-treated with 20 μ M MG-132 for
1072 6 hr. **(J)** Immunoblot analysis of total ubiquitination of Flag-tagged SLC3A2 following co-
1073 immunoprecipitating of SLC3A2 with anti-Flag antibody from lysates of HEK293T cells co-
1074 transfected with indicated plasmids.

1075 **Figure 8. NEDD4L regulates DSS-induced colitis through ferroptosis.**

1076 *Nedd4^{fl/fl}Villin^{Cre}* and *Nedd4^{fl/fl}* mice pre-treated with ferrostatin-1 (Fer1, 5 μ M/Kg) or DMSO
1077 were administered with 2% DSS for 5 days, and on the 9th day the mice were sacrificed for
1078 collecting colonic tissues and IECs. *Nedd4^{fl/fl}*+DMSO n=3, *Nedd4^{fl/fl}Villin^{Cre}*+DMSO n=4,
1079 *Nedd4^{fl/fl}*+Fer-1 n=6, *Nedd4^{fl/fl}Villin^{Cre}*+Fer-1 n=4. **(A)** Body weight change, **(B)** colon length,
1080 **(C)** gross morphology images, **(D)** histological score, **(E)** representative H&E staining, and
1081 **(F)** TUNEL staining of the colon sections from the indicated mice. **(G-J)** In a separate
1082 experiment, the IECs and colon tissues from mice treated as in **(A)** were subjected to flow
1083 cytometer analysis of EpCAM, CD45, and PI staining **(G, H)**, 4-HNE IHC staining **(I)**, and
1084 ZO-1 IF staining **(J)**. **(K)** qPCR analysis, **(L)** western blotting analysis, and **(M)** protein
1085 intensity analysis of the indicated proteins of IECs treated as in **(A)**. *Nedd4^{fl/fl}*+DMSO n=3-
1086 5, *Nedd4^{fl/fl}Villin^{Cre}*+DMSO n=3, *Nedd4^{fl/fl}*+Fer-1 n=4-6, *Nedd4^{fl/fl}Villin^{Cre}*+Fer-1 n=3-5, as
1087 indicated in the figure. Scale bar, 50 μ m.

1088 Data represent mean \pm SEM from at least two independent experiments. Each dot means
1089 independent samples. ns, no significant difference. *P<0.05, **P<0.01. Statistical analysis
1090 was performed using a two-way ANOVA test in **A**, 1-way ANOVA multiple comparisons **B**,
1091 **D, G, H, K, and M**.

1092 **Figure 9. *Nedd4l* deficiency in IECs promotes AOM/DSS-induced colorectal cancer**
1093 **in mice.**

1094 **(A)** MRI images of *Nedd4^{fl/fl}Villin^{Cre}* and *Nedd4^{fl/fl}* mice treated with AOM/DSS for 90 days.
1095 **(B-D)** Tumor numbers (*Nedd4^{fl/fl}* n=15, *Nedd4^{fl/fl}Villin^{Cre}* n=21) **(B)**, tumor size (n=6/group)
1096 **(C)**, and representative morphology images of colons **(D)** from the AOM/DSS-treated mice
1097 on day 90. **(E-G)** Representative IHC staining of sections from the tumor, adjacent tumor,
1098 and distal normal tissues of AOM/DSS-treated *Nedd4^{fl/fl}Villin^{Cre}* and *Nedd4^{fl/fl}* mice with anti-
1099 Ki67 antibody **(E)**, anti-4-HNE antibody **(F)**, and **(G)** statistical analysis of Ki67 positive cells

1100 according to (n=4/group) **(E)**. **(H-L)** Schematic diagram of the treatment plan for AOM/DSS-
1101 treated *Nedd4^{fl/fl}Villin^{Cre}* and *Nedd4^{fl/fl}* mice with ddH₂O or DFOM**(H)**. Representative
1102 morphology images of colons **(I)**, tumor numbers**(J)**, statistical analysis of 4-HNE IHC
1103 staining score **(K)**, and representative images of 4-HNE IHC staining from the treated mice
1104 as in **(I)**. *Nedd4^{fl/fl}+ddH₂O* n=5, *Nedd4^{fl/fl}Villin^{Cre}+ddH₂O* n=5, *Nedd4^{fl/fl}+DFOM* n=8,
1105 *Nedd4^{fl/fl}Villin^{Cre}+DFOM* n=8. Scale bars, 50 μm.

1106 Data represent mean ± SEM from at least two independent experiments. Each dot means
1107 independent samples. ns, no significant difference. ***, P<0.001; **, P<0.01; *, P<0.05.
1108 Statistical analysis was performed using a 2-tailed Student's t-test in **B**, **C**, and **F**, and 1-
1109 way ANOVA multiple comparisons in **J**, and **K**.

1110 **Figure 10. Expression of NEDD4L is significantly down-regulated in IECs of patients**
1111 **and mice with colorectal cancer.**

1112 **(A-D)** Wild-type mice were treated with AOM/DSS, and the IECs (on day 0, day 15, and
1113 day 60) and tumor nodules (on day 90) were collected for immunoblot analysis **(A)**, protein
1114 intensity analysis**(B)**, qPCR analysis **(C)**, and **(D)** correlative analysis of the indicated
1115 proteins. n=3/group. **(E, F)** Representative NEDD4L and 4-HNE IHC staining of sections
1116 from the tumor, adjacent tumor, and distal normal tissues of patients with colorectal cancer
1117 **(E)**, and statistical analysis of NEDD4L and 4-HNE IHC staining intensity **(F)** according to
1118 **(E)**. (n=55) **(G, H)**. Representative SLC3A2, GPX4, and NEDD4L IHC staining sections
1119 from the tumor tissues of patients with colorectal cancer **(G)**, and correlative analysis
1120 between SLC3A2, GPX4, and NEDD4L IHC staining intensity score (n=55) **(H)**. Scale bars,
1121 50 μm.

1122 Data represent mean ± SEM from at least two independent experiments. Each dot means
1123 independent samples. ns, no significant difference. ***, P<0.001; **, P<0.01; *, P<0.05.
1124 Statistical analysis was performed using 1-way ANOVA multiple comparisons in **B**, **C**, and
1125 **F**, and a Pearson correlation test in **D** and **H**.

1126

1127

1128

1129

Table1 NEDD4L expression in patients with UC from Xijing Hospital

1130

NEDD4L

1131

1132

1133

1134

1135

1136

1137

1138

Table2 NEDD4L expression in patients with UC and CD from FAHZU Hospital

1139

NEDD4L

1140

1141

1142

1143

1144

Group types	Total No. studied	NEDD4L			
		-	+	++	+++
		%	%	%	%
Normal	40	4(10%)	2(5%)	26(65%)	8(20%)
Ulcerative colitis	83***	32(38.5%)	10(12.1%)	37(44.6%)	4(4.8%)

Note: Correlations were analyzed using Pearson's χ^2 test.

*** $P < 0.001$ compared with normal tissues.

Group types	Total No. studied	NEDD4L			
		-	+	++	+++
		%	%	%	%
Normal	31	0(0%)	0(0%)	1(3.2%)	30(96.8%)
Ulcerative colitis	36***	1(2.8%)	2(5.6%)	19(52.8%)	14(38.8%)
Crohn's disease	41***	0(0%)	1(2.4%)	24(58.6%)	16(39%)

Note: Correlations were analyzed using Pearson's χ^2 test.

*** $P < 0.001$ compared with normal tissues.

Figure 1

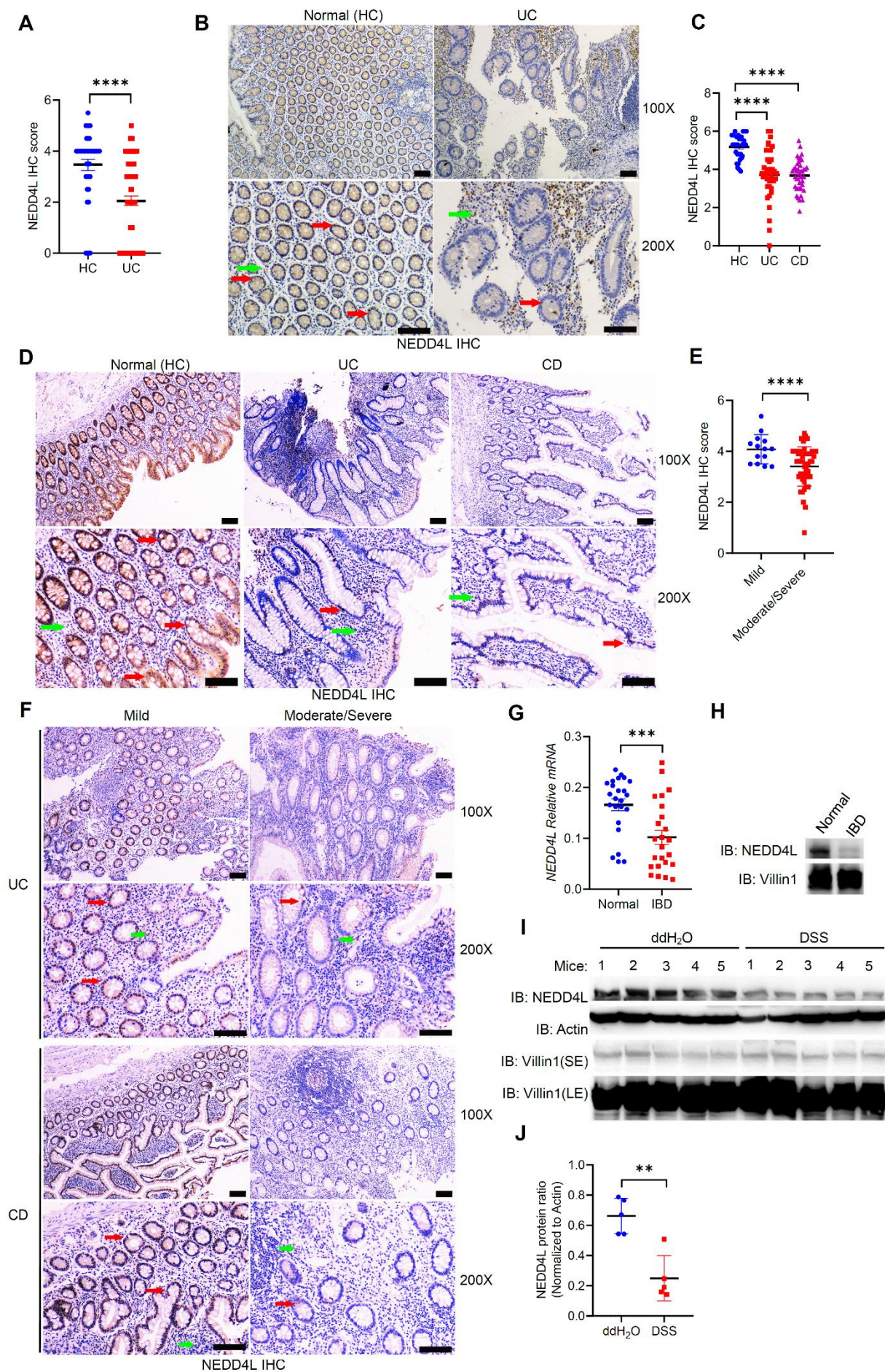


Figure 2

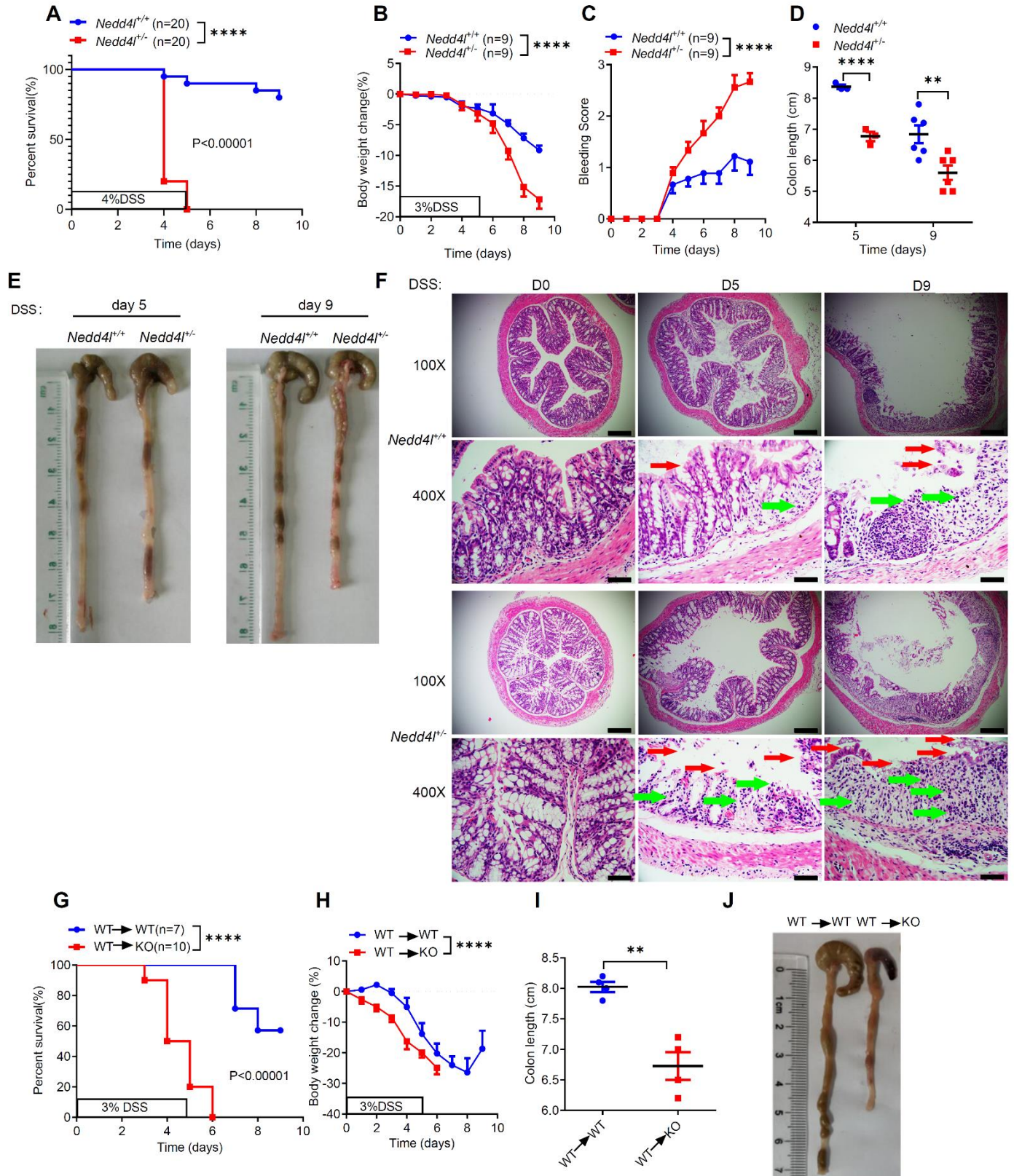


Figure 3

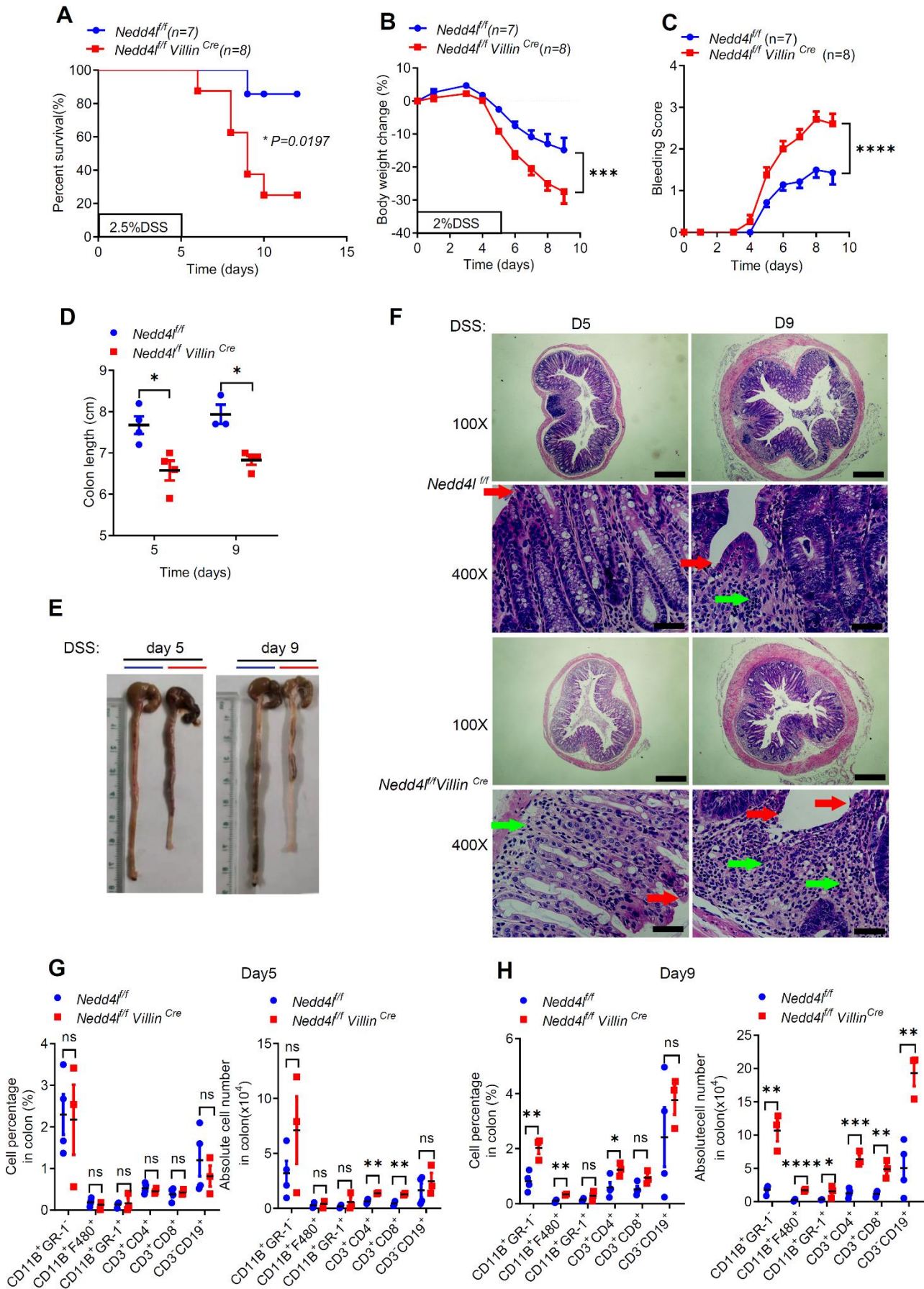


Figure 4

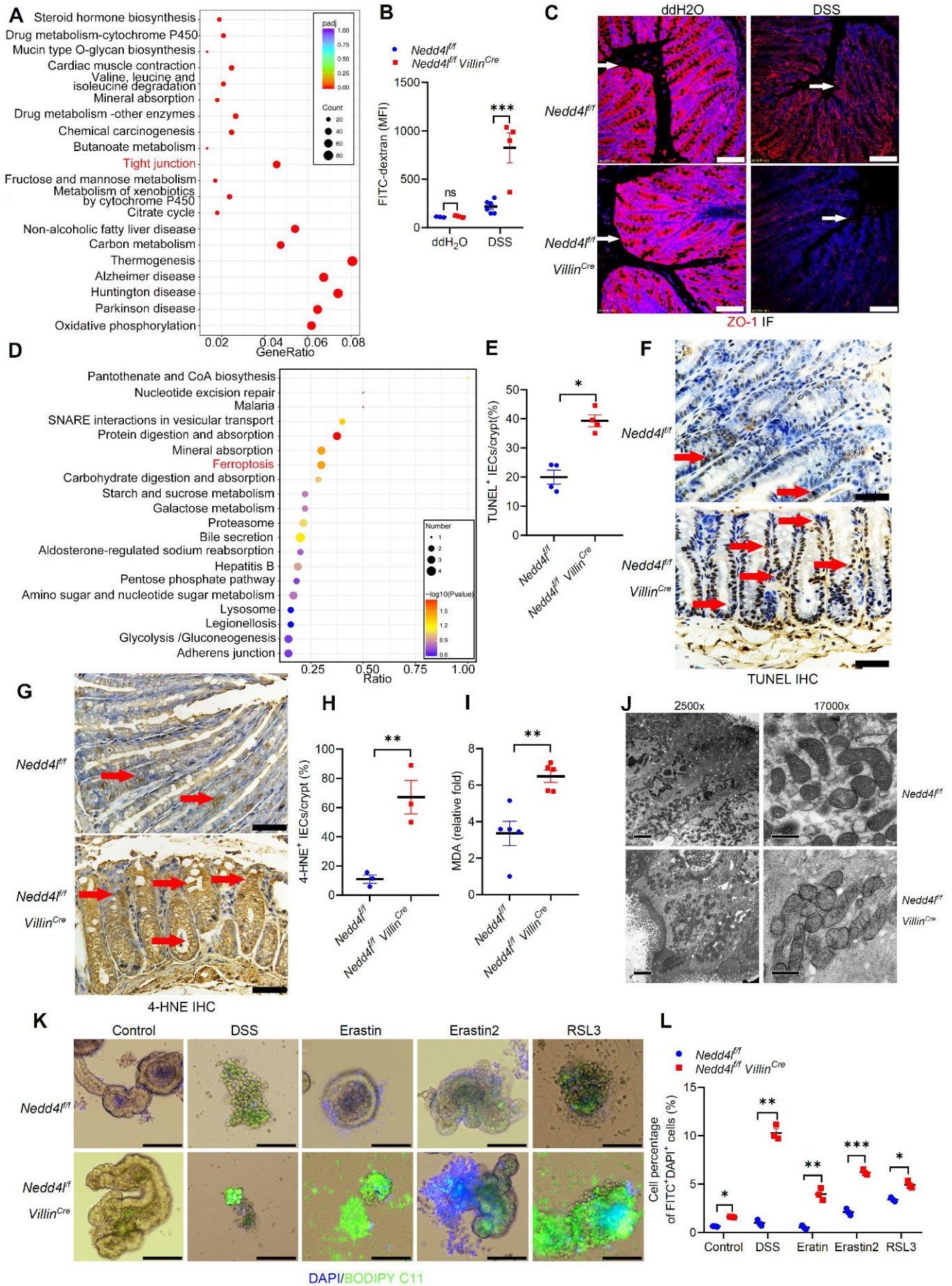


Figure 5

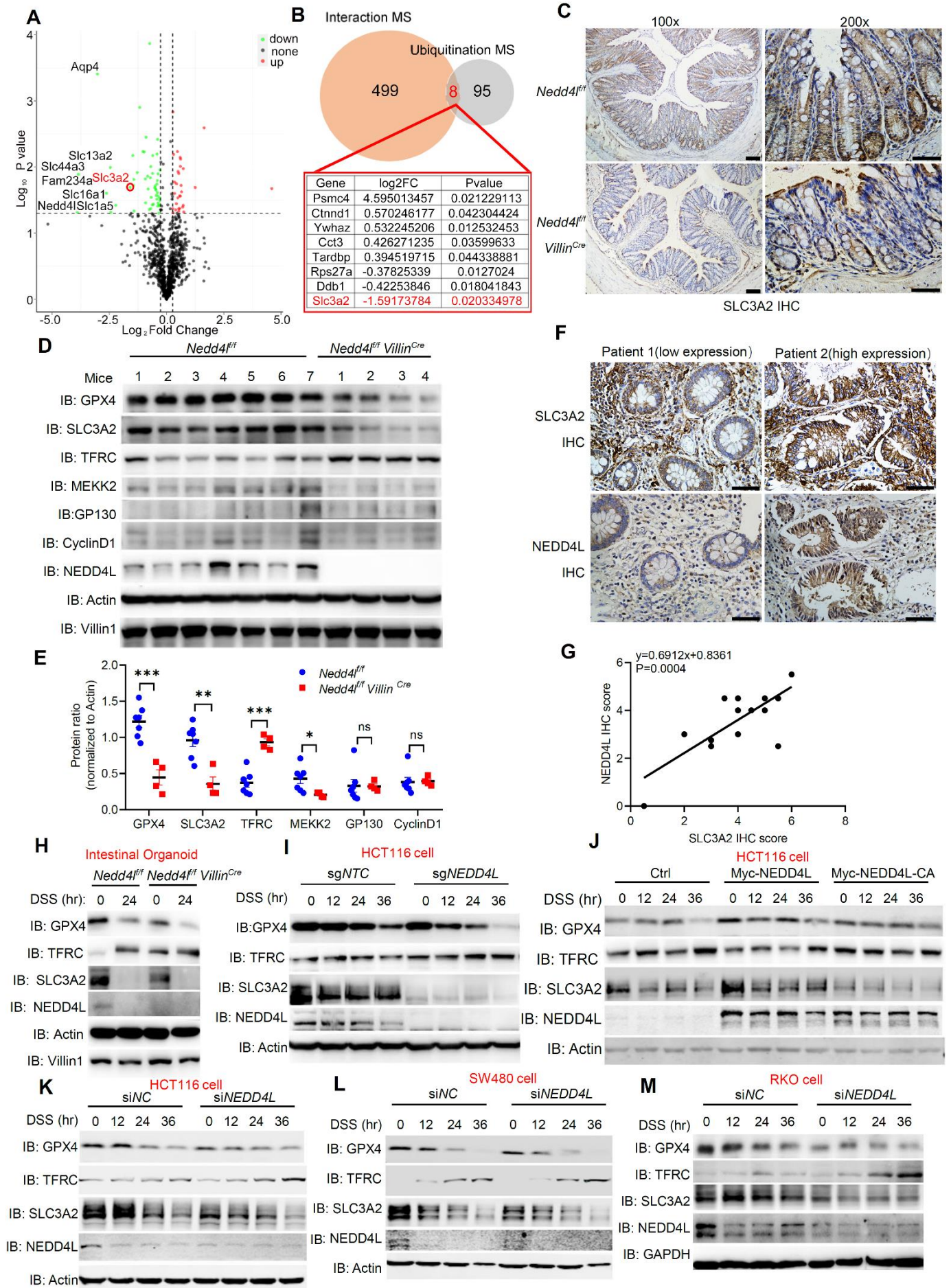


Figure 6

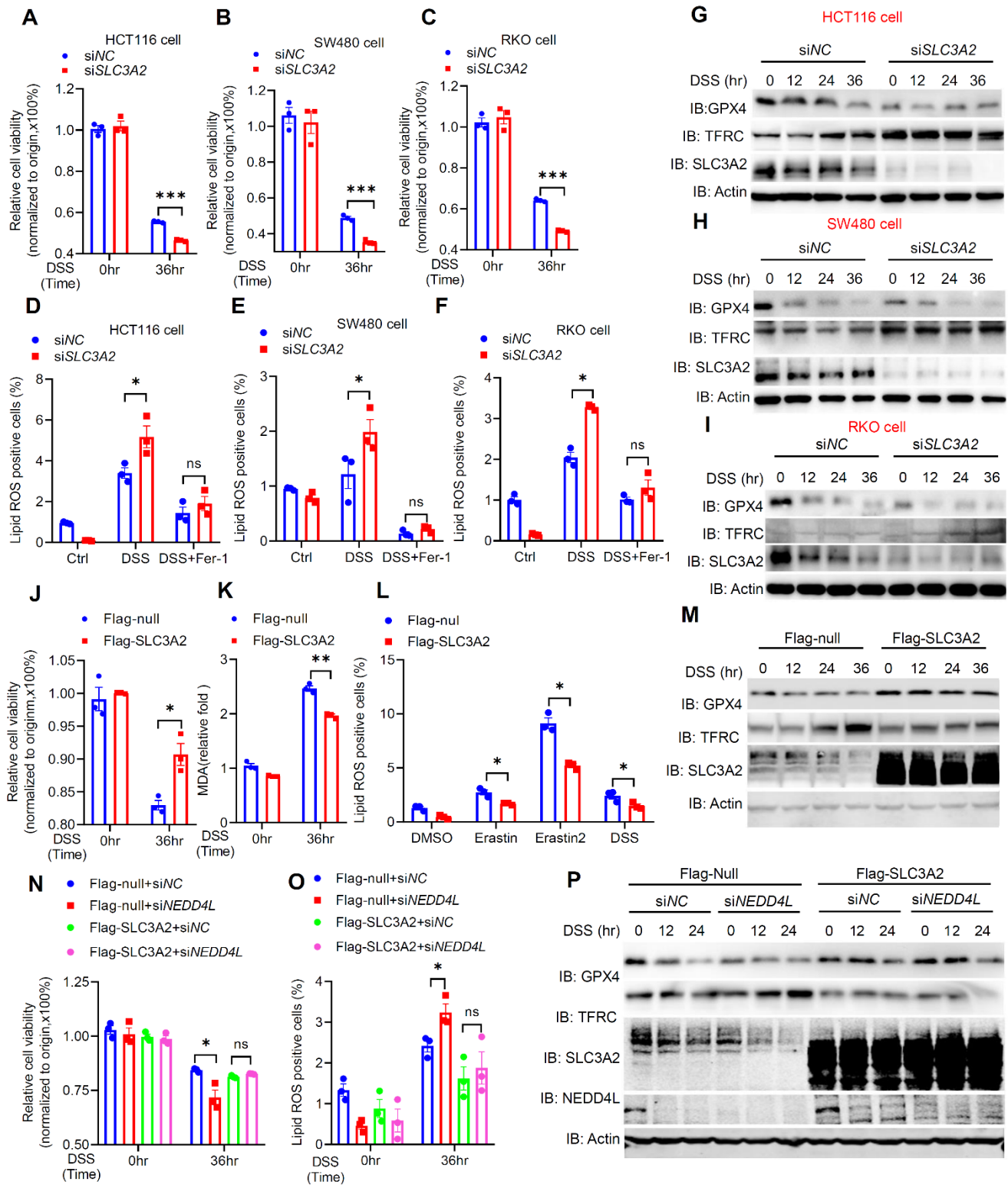


Figure 7

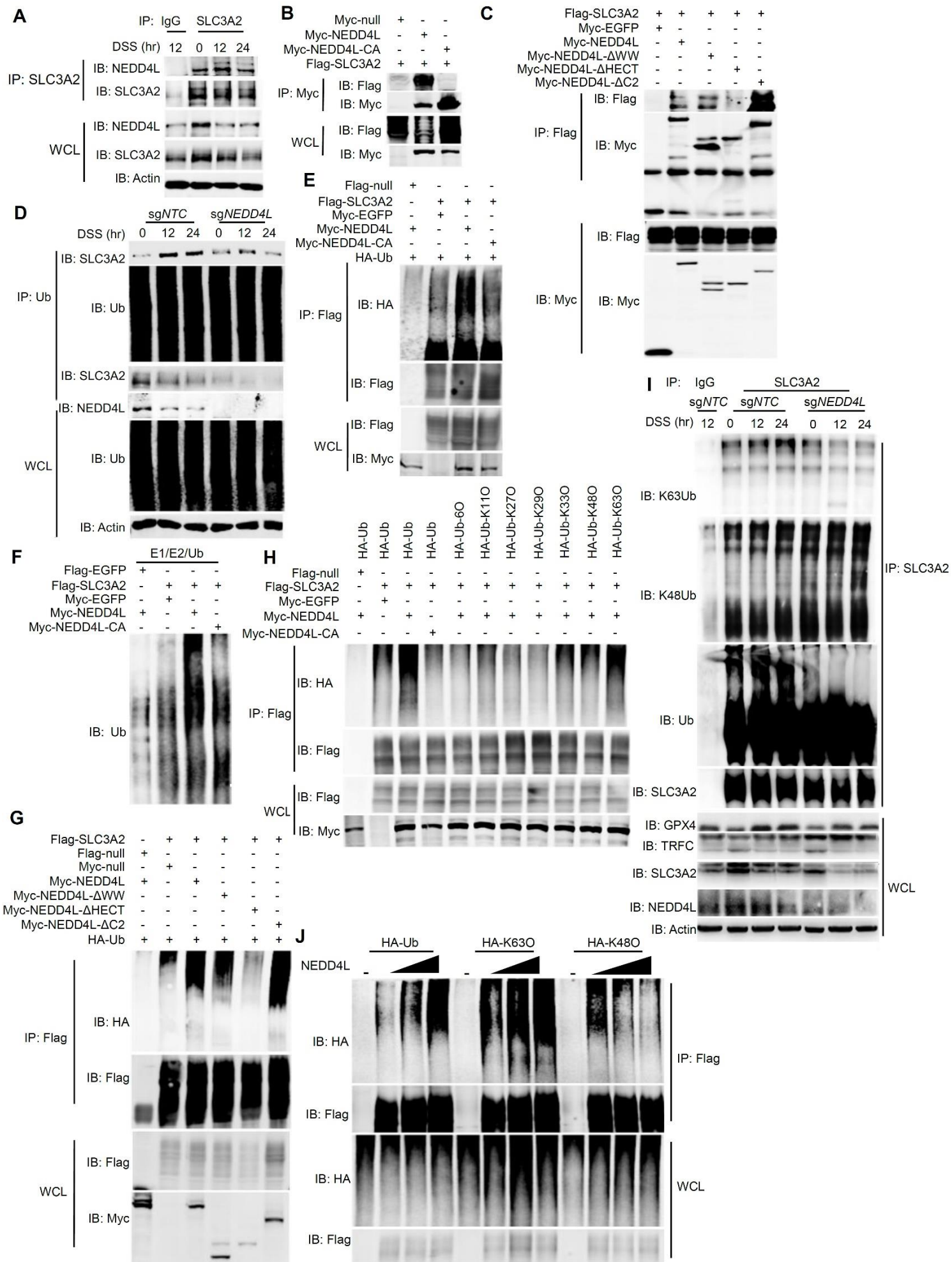


Figure 8

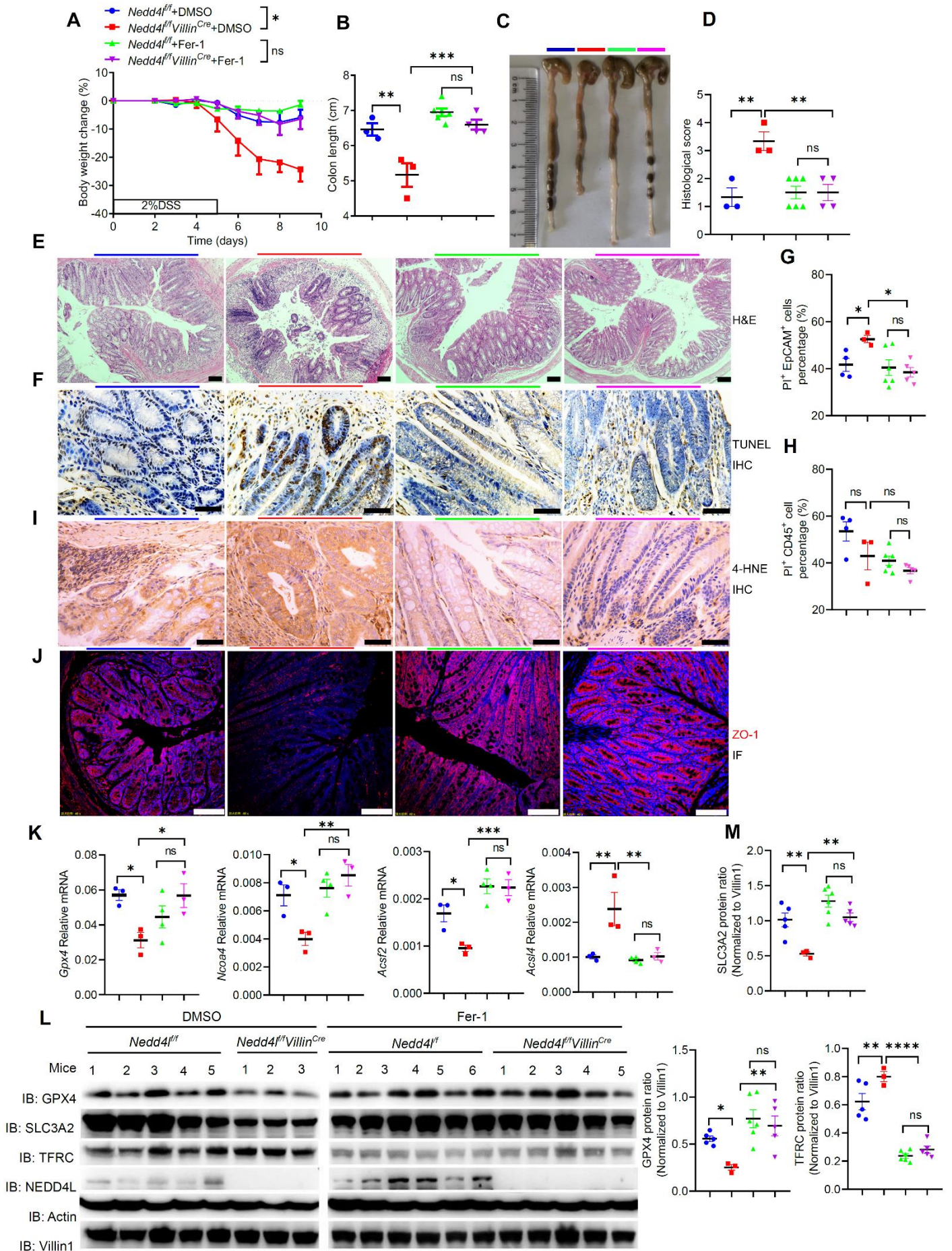


Figure 9

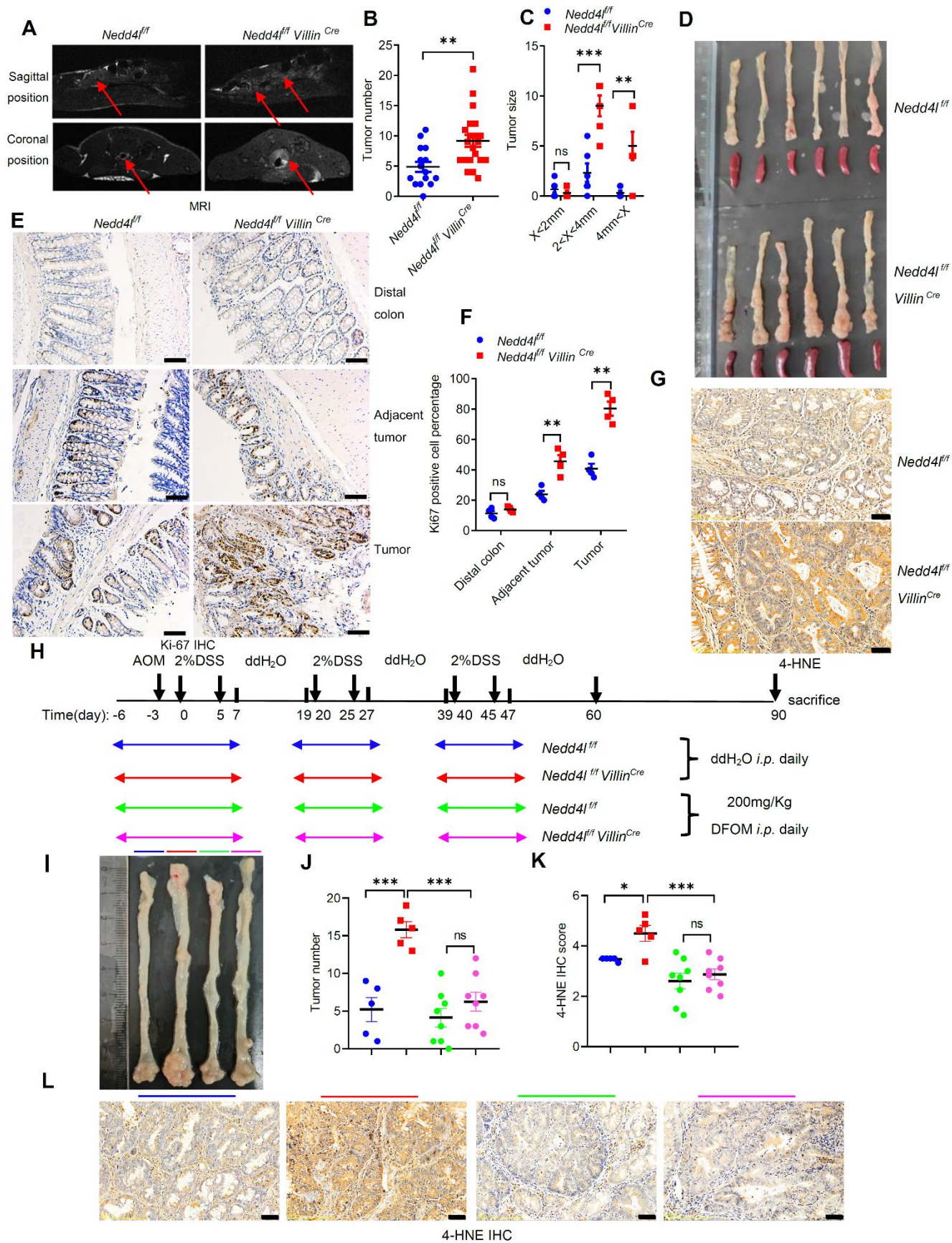


Figure 10

